Title: Diverse functions of retinoic acid in brain vascular development

Authors: Stephanie Bonney[1,6], Susan Harrison-Uy[2,6], Swati Mishra[1], Amber MacPherson[1], Youngshik Choe[2,5], Dan Li[3], Shou-Ching Jaminet[3], Marcus Fruttiger[4], Samuel J. Pleasure[2], and Julie A. Siegenthaler[1,7]

Author Affiliations: [1]Department of Pediatrics, Section of Developmental Biology, University of Colorado, School of Medicine-Anschutz Medical Campus Aurora, CO 80045 USA. [2]Department of Neurology, UC San Francisco, San Francisco, CA 94158 USA; [3]Beth Israel Deaconess Medical Center, Department of Pathology, Harvard Medical School Boston, MA 02215 USA; [4]Institute of Ophthalmology–Cell Biology, University College London, London EC1V 9EL, England, UK; [5]Current address: Department of Neural Development and Disease, Korea Brain Research Institute, Daegu, 701-300 Korea.

[6]Co-first authors

[7]Corresponding Author:

Julie A. Siegenthaler, PhD

University of Colorado, School of Medicine-Anschutz Medical Campus

Department of Pediatrics

12800 East 19th Ave MS-8313

Aurora, CO 80045

E-mail: julie.siegenthaler@ucdenver.edu

Abbreviated title: Retinoic acid in neurovascular development

Figures: 9 Pages: 39 Abstract: 239 words Introduction: 647 words Discussion: 1500 words

Acknowledgments: The authors declare no competing financial interests. This work was supported by the following funding agencies: National Institutes of Health/National Institute of Neurological Disorders and Stroke [K99-R00 NS070920 to J.A.S], American Health Association/American Academy of Neurology [Lawrence M. Brass, M.D. Stroke Research Postdoctoral Fellowship to J.A.S.] and National Institutes of Health/National Institute on Drug Abuse [R01 DA017627 to S.J.P.]. J.A.S. would like to recognize the invaluable guidance and support of Virginia Lancaster and Dr. Joseph Gerber throughout her life and career.

Abstract (239 words)

As neural structures grow in size and increase metabolic demand, the central nervous system (CNS) vasculature undergoes extensive growth, remodeling, and maturation. Signals from neural tissue act on endothelial cells to stimulate blood vessel ingression, vessel patterning and acquisition of mature brain vascular traits, most notably the blood brain barrier (BBB). Using mouse genetic and *in vitro* approaches, **we identified retinoic acid (RA) as an important regulator of brain vascular development via non-cell and cell autonomous regulation of endothelial WNT signaling**. **Our analysis of globally RA-deficient embryos (*Rdh10* mutants) points to an important, non-cell autonomous function for RA in development of the vasculature in the neocortex.** We demonstrate *Rdh10* mutants have severe defects in cerebrovascular development and this phenotype correlates with near absence of endothelial WNT signaling specifically in the cerebrovasculature and substantially elevated expression of WNT inhibitors in the neocortex. We show RA can suppress expression of WNT inhibitors in neocortical progenitors. **Analysis of vasculature in non-neocortical brain regions suggested RA may have a separate, cell-autonomous function in brain endothelial cells to inhibit WNT signaling.** Using both gain and loss of RA signaling approaches, we show RA signaling in brain endothelial cells can inhibit WNT-β-catenin transcriptional activity and this is required to moderate expression of WNT target Sox17. **From this, a model emerges where RA acts upstream of the WNT pathway via non-cell and cell autonomous mechanisms to ensure formation of an adequate and stable brain vascular plexus.**

Significance (114 words)

Work presented here provides novel insight into important yet little understood aspects of brain vascular development and our experiments place, for the first time, a factor upstream of endothelial WNT signaling. We show RA is permissive for cerebrovascular growth via suppression of WNT inhibitor expression in the neocortex. RA also functions cell-autonomously in brain endothelial cells to modulate WNT signaling and its downstream target Sox17. The significance of this is that though endothelial WNT signaling is required for neurovascular development, too much endothelial WNT signaling, as well as over-expression of its target Sox17, are detrimental. Thus RA may act as a 'brake' on endothelial WNT signaling and Sox17 to ensure normal brain vascular development.

Introduction (647 words)

Expansion and maturation of the vasculature is essential to support brain growth and establish a vascular plexus that can sustain brain function. Mouse CNS vascular development begins at ~embryonic day 9 (E9) when vessels from the perineural vascular plexus (PNVP) that surround the CNS ingress starting at the spinal cord and soon after in more rostral brain structures (Nakao et al., 1988). Angiogenic growth occurs in response to vascular endothelial growth factor-A (VEGFA) (Breier et al., 1992; Haigh et al., 2003; Raab et al., 2004; James et al., 2009) and WNT ligands (Stenman et al., 2008; Daneman et al., 2009) secreted by neural progenitors in the ventricular zone (VZ) and, later, WNT ligands from post-mitotic neurons. Parallel with vascular growth, CNS endothelial cells (ECs) acquire blood brain barrier (BBB) properties including expression of tight junctional proteins and transporters like glucose transporter-1 (GLUT-1) that ensure influx and efflux of substances across the BBB (Bauer et al., 1993; Daneman et al., 2010). CNS vascular development is complex, in part because vascular growth and maturation occur against the backdrop of a rapidly changing neural environment that produces most neuro-angiogenic ligands. How CNS ECs successfully integrate diverse angiogenic and maturation cues from the neural environment to create a stable vasculature is not well understood.

Retinoic acid (RA) is a lipid soluble hormone produced by cell types within and around the CNS and it has diverse developmental roles (Napoli, 1999; Toresson et al., 1999; Li et al., 2000; Maden, 2001; Schneider et al., 2001; Smith et al., 2001; Zhang et al., 2003; Siegenthaler et al., 2009). RA signaling is mediated by Retinoic acid receptors (RARs) that act as receptors and transcription factors to control gene transcription (Al Tanoury et al., 2013). RA is required for vasculogenesis in the early embryo (Lai et al., 2003; Bohnsack et al., 2004) and there is some evidence that RA may have a role in angiogenesis and vessel maturation in the CNS. RA is implicated in BBB development through regulation of BBB protein expression, specifically VE-Cadherin (Mizee et al., 2013; Lippmann et al., 2014). Mice that lack both retinoid receptors RARα and RARγ have significant defects in CNS

development and visible brain hemorrhaging, notably in the cerebral hemispheres (Lohnes et al., 1994). RAR receptors are expressed in fetal human and mouse brain ECs (Mizee et al., 2013), suggesting that ECs in the developing CNS are RA-responsive. Collectively these data indicate RA may have a significant role in controlling brain vascular development.

Using global RA-deficient mouse mutants (*Rdh10* mutants) and EC-specific disruption of RA signaling (*PdgfbiCre; dnRAR403-flox*), **we show RA has separate, non-cell and cell-autonomous roles with regard to endothelial WNT signaling.** *Rdh10* mutant embryos have impaired neocortical development (Siegenthaler et al. 2009) and here we describe vascular growth defects specific to the neocortex. Reduced cerebrovascular growth in *Rdh10* mutants is accompanied by disruption in VEGF-A and WNT. However, elevated *Vegfa* expression is not limited to the neocortex and may reflect widespread brain hypoxia. In contrast, endothelial WNT signaling is specifically diminished in the *Rdh10* mutant cerebrovasculature. This is accompanied by significantly elevated levels of WNT inhibitors in the *Rdh10* mutant neocortex but no other brain regions. **Combined with our data showing RA suppresses gene expression of WNT inhibitors in cultured neocortical progenitors, our analysis of cerebrovascular defects in *Rdh10* mutants point to RA functioning non-cell autonomously in the neocortex to create a permissive environment for endothelial WNT signaling.** Vascular development is relatively normal in other regions of *Rdh10* mutant brains and, strikingly, endothelial WNT signaling is increased. **This finding suggested RA may act cell-autonomously in brain ECs to inhibit WNT signaling. In support of this, we find *PdgfbiCre; dnRAR403-flox* mutants have increased endothelial WNT signaling and expression of WNT transcriptional targets LEF-1 and Sox17. Collectively, this work shows that RA regulates brain vascular development by acting upstream of WNT signaling through different, non-cell and cell autonomous mechanisms.**

Materials and Methods

Animals. Mice used for experiments here were housed in specific-pathogen-free facilities approved by AALAC and were handled in accordance with protocols approved by the UCSF Committee on Animal Research and the UC Anschutz Medical Campus IACUC committee. The following mouse lines were used in this study: *PdgfbiCre* (Claxton et al., 2008), *Ctnnb1-flox* (Brault et al., 2001), *Bat-gal-lacZ* (Maretto et al., 2003), *Ephrin-B2-H2B-GFP* (Davy et al., 2006), and *dnRAR403-flox* (Rosselot et al., 2010). The *Rdh10* ENU point mutation mutant allele has been described previously (Ashique et al., 2012) and were obtained from Andy Peterson at Genentech. Tamoxifen (Sigma) was dissolved in corn oil (Sigma; 20 mg/ml) and 100 ul was injected intra-peritoneal into pregnant females at E9 and E10 to generate *PdgfbiCre; dnRAR403-flox* mutant animals. For generation of *PdgfbiCre; Ctnnb1-fl/fl* mutants, tamoxifen was administered to pregnant females on E11 and E12. RA-enriched diet (final concentration 0.175 mg/g food) consisted of *all-trans*-RA (atRA; Sigma-Aldrich) dissolved in corn oil and mixed with Bioserv Nutra-Gel Diet™, Grain-Based Formula, Cherry Flavor. atRA diet was prepared fresh daily and provided ad libitum from the afternoon of E10 through the day of collection (E14.5 or E16.5).

Immunohistochemistry. Fetuses (E12.5-E18.5) were collected and whole heads or brains were fixed overnight in 4% paraformaldehyde. All tissues were cryoprotected with 20% sucrose in PBS and subsequently frozen in OCT. Tissue was cryosectioned in 12 μm increments. Immunohistochemistry was performed on tissue sections as described previously (Zarbalis et al., 2007; Siegenthaler et al., 2009) using the following antibodies: rabbit anti-β-galactosidase 1:500 (Cappel), rabbit anti-GLUT-1 1:500 (Lab Vision-Thermo Scientific), goat anti-Sox17 1:100 (R&D Systems), chicken anti-GFP 1:500 (Invitrogen), mouse anti-BrdU 1:50 (BD Biosciences) mouse anti-CoupTFII 1:100 (R&D Systems), rabbit anti-Claudin-3 1:200 (Invitrogen), rabbit anti-LEF-1 1:100 (Cell Signaling Technology), rabbit anti-Pax6 1:200 (Biolegend), chicken anti-Tbr2 1:100 (Millipore) and rat anti-Ctip2 1:1000 (Abcam).

Following incubation with primary antibody(s), sections were incubated with appropriate Alexafluor-conjugated secondary antibodies (Invitrogen), Alexafluor 633-conjugated isolectin-B4 (Invitrogen), and DAPI (Invitrogen). For LEF-1, immunostaining was performed using the Tyramide System Amplification (TSA) Kit (Invitrogen) per manufacturer's instructions. Immunofluorescent (IF) images were captured using a Retiga CCD-cooled camera and associated QCapture Pro software (QImaging Surrey, BC Canada), a Nikon i80 research microscope with Cool-Snap CCD-cooled camera or Zeiss 780 LSM confocal microscope.

Cell proliferation and trans-well migration assay with bEnd.3 cell line. The mouse brain endothelioma cell line (bEnd.3) was from ATCC (cat# CRL-2299). All experiments were performed on cells from passages 2-4 and cells were grown in Dulbecco's minimal essential media with 4.5g/L glucose, 1.5g/L sodium bicarbonate, 4mM L-glutamine (Invitrogen), 10% fetal bovine serum (FBS) (Invitrogen) and Penicillin (0.0637g/L)-Streptomycin (0.1g/L) (UCSF Cell Culture Facility or Invitrogen). On day 1 of the cell proliferation assays, $7x10^4$ cells were plated in each well of an 8-well glass chambered slide (Nunc Lab-Tek) and allowed to adhere for ~5 hours after which media was changed to DMEM with 1% FBS. On day 2, atRA (50 nM; Sigma-Aldrich) and/or WNT3a (0.05, 0.1 or 0.3 µg/ml; R&D Systems) was added to the media. On day 5, 1 mM BrdU (Roche) was added to the media in each well and 2 hours later, cells were fixed for 15 min with 4% paraformaldehyde. Cells were immunostained to detect BrdU incorporation (mouse anti-BrdU 1:50; BD Bioscience) and stained with DAPI to visualize all cell nuclei. For analysis of cell proliferation, 4, 10x images were obtained for each treatment condition (2 wells per treatment in each replicate) and the percentage of BrdU+ cells was determined for each image (# BrdU+ cells/# DAPI+ cells). The value for each replicate is an average from the four images. For the transwell migration assay, $8x10^4$ cells in 100 µl of media was pipetted into the top chamber of a Millicell cell culture insert with a 8µm filter pore size (Millipore cat#: PI8P01250). The culture well immediately below the insert contained 500 µl of media with retinoic acid (50 nM) and/or WNT3a (0.1

or 0.3 μg/ml) and WNT7a (5 μg/ml). The cells were allowed to migrate through the pores for 20 hours, cells were fixed for 15 minutes with 4% paraformaldehyde and a cotton swab was used to remove the cells still within the top chamber. The filter was cut away from the insert, stained with DAPI to visualize the cell nuclei and filters were mounted onto slides for imaging. For analysis of cell migration, 4, 10x images were obtained for each treatment condition (2 transwell filters per treatment in each replicate) and the number of DAPI+ nuclei were assessed in a counting area within each 10x image field. For WNT7a-RA experiments, the entire 10x field was counted. For both the cell proliferation and transwell migration assays, a minimum of three independent replicates (n≥3) were performed for each treatment condition.

Quantitative analysis of fetal neurovasculature. Vessel density and β-gal+ endothelial cell analysis was performed on E12.5 and E14.5 control (*Rdh10*$^{+/+}$ or *Rdh10*$^{+/-}$) and *Rdh10*-mutant animals (thalamus, midbrain and hindbrain), E14.5 and E16.5 *Bat-gal-LacZ/+* animals (forebrain), and E18.5 *PdgfbiCre; dnRAR403-fl* control and mutant animals (forebrain) on a minimum of three separate brains per genotype/treatment/embryonic day point (n≥3). To determine mean vessel density, the sum length of IB4+ cerebral vessels was determined from a single, 20x field and divided by the area of the tissue analyzed. All density measurements were performed using ImageJ software (NIH) on a minimum of 5, 20x fields per brain. For quantification of β-gal+ ECs in fetuses expressing the *Bat-gal-lacZ/+* allele, the number of β-galactosidase+/IB4+ ECs was counted in a single, 20x image and divided by the sum length of IB4+ blood vessels within the image. This was performed on a minimum of 5, 20x fields per brain. To quantify cell proliferation in the *Rdh10* E14.5 control and mutant PNVP and in the neocortical plexus, pregnant dams were injected with (50 mg/kg body weight, Roche) BrdU and embryos were collected 2 hours later. Following processing for GLUT-1/BrdU/Ib4/DAPI IF, the total number of BrdU+/GLUT-1+ ECs was divided by the total number of GLUT-1+ ECs in a 20x field. Analysis was performed separately for the PNVP and vessels with the neocortical plexus. All cell proliferation

analysis was performed using ImageJ software (NIH) on a minimum of 5, 20x fields per brain. Cell proliferation analysis was performed on a minimum of 3 separate brains per genotype ($n \geq 3$).

Luciferase assays. HEK293 cells were grown in 1:1 DMEM:F12 supplemented with 10% FBS and penicillin:streptomycin. Twenty-four hours prior to transfection cells, were plated in antibiotic free media at a density of $4x10^5$ per well of poly-l-lysine treated 12 well plates. Cells were transfected using Lipofectamine 2000 (Invitrogen) with 500ng of the expression plasmids: RARα.pCMV-Sport6 (Open Biosystems), RXRβ.pCMV-Sport6 (Open Biosystems) or dnRARα.pCIG (subcloned with dnRARa403 (Addgene plasmid: 15153) and pCIG (Megason and McMahon, 2002)) and 100 ng of the reporter plasmids M50-TOP-Flash or M51-FOP-Flash (Addgene). pCIG was added to normalize total DNA concentration. Four hours following transfection cells were treated with recombinant mouse WNT3a (0.1 μg/ml; R&D Systems), retinoic acid (1 μM; Sigma Aldrich) or vector control. Luciferase levels were measured 18 hours post-transfection using the Dual Luciferase Assay Kit according to the manufacturer's instructions (Promega). Luciferase assays were performed in triplicate and normalized to total protein concentration. All assays were repeated in 3 independent experiments, and the results of one such experiment are shown in Figure 5.

Microvessel isolation, multi-gene transcriptional profiling. Isolation of RNA from microvessels from E18.5 control (*PdgfbiCre/+;Ctnnb1-fl/+*) and mutant (*PdgfbiCre/+; Ctnnb1-fl/fl*) brains was performed as described previously (Siegenthaler et al., 2013). Multigene transcriptional profiling, a form of quantitative RT-PCR, was used to determine the number of mRNA copies per cell normalized to 18S rRNA abundance (10^6 18S-rRNA copies/cell) (Shih and Smith, 2005). For each sample, mRNA copy numbers for *Sox17*, *Lef1* and *Axin2* were normalized to *CD144* copy number to correct for variability in microvessel isolation between brains. Analysis was performed on microvessels isolated from 3 control and 3 mutant E18.5 brains (n=3). For RT-PCR of RA receptor gene expression, RNA was isolated from

E18.5 wildtype microvessels and postnatal day 7 meninges and cDNA was generated from 100 ng of RNA using SuperScript® VILO™ cDNA Synthesis Kit (Invitrogen). Primer sequences are as follows: *Lef1* forward: AGGGCGACTTAGCCGACAT, *Lef1* reverse: GGGCTTGTCTGACCACCTCAT; *Axin2* forward: GTGCCGACCTCAAGTGCAA, *Axin2* reverse: GGTGGCCCGAAGAGTTTTG; *Sox17* forward: GGCCGATGAACGCCTTTAT, *Sox17* reverse: AGCTCTGCGTTGTGCAGATCT; *Rara* forward: AGCTCTGCGTTGTGCAGATCT, *Rara* reverse: AGAGTGTCCAAGCCCTCAGA; *Rarb* forward: TTCAAAGCAGGAATGCACAG, *Rarb* reverse: GGCAAAGGTGAACACAAGGT; *Rarg* forward: CACAGCCTGCCAGTCTACAA, *Rarg* reverse: CTGGCAGAGTGAGGGAAAAG; *Rxra* forward: CTGCCGCTCGACTTCTCTAC, *Rxra* reverse: ATATTTCCTGAGGGATGGGC; *Rxrb* forward: TGGGGGTGAGAAAAGAGATG, *Rxrb* reverse: GAGCGACACTGTGGAGTTGA; *Rxrg* forward: AATGCTCTTGGCTCTCCGTA, *Rxrg* reverse: TGAAGAAGCCTTTGCAACCT.

Tissue and neocortical progenitor cell culture/isolation, qPCR. Meninges were removed from E14 wild-type (n=5) and *RDH10* mutant brains (n=4). RNA was isolated separately from the neocortices and the non-neocortical brain regions using the RNeasy Mini Kit (Qiagen). E14 cortical progenitor cells (R&D systems) were seeded onto 15µg/ml Poly-L-ornithine (Sigma) and 1µg/ml laminin (Sigma) coated 6 well plates as a monolayer culture. Cell culture medium was composed of DMEM/F-12 with glutamax (Life Technologies), 1X N2 supplement composed of Insulin, Human Transferrin, Putrescine, Selenite and Progesterone (Life Technologies) and glucose (Sigma). Culture medium was supplemented with 10ng/ml of human basic fibroblast growth factor (R&D systems) and 10ng/ml of human epidermal growth factor (R&D systems) every day until cell lysate collection to maintain cortical progenitors cells in an undifferentiated state. After 24 hours exposure to treatment conditions, total cellular RNA was isolated from vehicle treated, 1µM atRA and 1µM atRA +1µM pan-Retinoic Acid Receptor antagonist (Santa Cruz Biotechnology) treated using the RNeasy Mini Kit. Experiments using cortical progenitor cells were performed three separate times (n=3). To synthesize cDNA, specifications were followed

using the iScript cDNA Synthesis Kit with 1 µg (brain samples) or 500 ng (cultured cells) of RNA from each sample. To assess *Vegfa*, *Ldha*, *Pdk*, *Cox4-2*, *Slc2a1*, *WNT7a*, *WNT7b*, *Sfrp1*, *Sfrp2*, *Sfrp4*, *Sfrp5* and *Dkk1* transcript levels qRT-PCR was performed according to the SYBR Green (BioRad) protocol using the BioRad CFX96 Real Time PCR Detection System. For an internal control, *Actb* transcript levels were also assessed. To identify differences in expression between control and mutant genotypes, delta-delta CT analysis was applied. Primer sequences are as follows: *Vegfa* forward: CAGGCTGCTGTAACGATGAA, *Vegfa* reverse: TTTGACCCTTTCCCTTTCCT; *Ldha* forward: AGCAGGTGGTTGAGAGTGCT, *Ldha* reverse: GGCCTCTTCCTCAGAAGTCA; *Pdk1* forward: CCCCGATTCAGGTTCACG, *Pdk1* reverse: CCCGGTCACTCATCTTCACA; *Cox4-2* forward: GGTTGTCACCCTGACGGAAG, *Cox4-2* reverse: GAGGGGAGGGGATGATTGTC ; *Slc2a1* forward: TCAGGCGGAAGCTAGGAAC, *Slc2a1* reverse: GGAGGGAAACATGCAGTCATC; *WNT7a* forward: GCAATAAGACAGCCCCTCAG, *WNT7a* reverse: ATCCTGCCTGTGATCTGACC; *WNT7b* forward: CAGCCAATCTTCCATTCCAT, *WNT7b* reverse: CCTGACCTCTCCTGAACCTG; *Sfrp1* forward: GAGTTTTGTTGCGGACCTGT, *Sfrp1* reverse: GCCAGGGACAAAGCTAATGA; *Sfrp2* forward: GCTTGTGGGTCCCAGACTTA, *Sfrp2* reverse: GCATCATGCAATGAGGAATG; *Sfrp4* forward: GACCCTGGCAACATACCTGA, *Sfrp4* reverse: CATCTTGATGGGGCAGGATA; *Sfrp5* forward: TGGAGCCCAGAAGAAGAAGA, *Sfrp5* reverse: TTCTTGTCCCAGCGGTAGAC; *Dkk1* forward: GCCTCCGATCATCAGACTGT, *Dkk1* reverse: GCTGGCTTGATGGTGATCTT; *Actb* forward: CTAGGCACCAGGGTGTGAT, *Actb* reverse: TGCCAGATCTTCTCCATGTC.

Immunoblots. Cortices (E18.5) from *PdgfbiCre; dnRAR403-fl* from four separate animals per genotype (n=4) were collected, lysed in RIPA buffer (Sigma) containing a protease inhibitor cocktail tablet (Roche). Protein concentration was determined using a BCA kit (Pierce). Lysates were combined with 4X sample buffer (300 mM Tris, 5% SDS, 50% glycerol, 0.025% bromophenol blue, 250 mM β-mercaptoethanol) and 70 ug (E18.5) or 15 ug (E16.5) of protein per sample was run on Protean Tris-HCI

4-20% gradient gel (Bio-Rad) then transferred onto PVDF membranes (Bio-Rad) or nitrocellulose membranes (Bio-Rad) using the Trans-Blot Turbo System (Bio-Rad). Immunoblots were blocked with 5% non-fat dehydrated milk (NFDM) in Tris buffered saline (TBS) with 0.1% Tween (TBS-T) for 1.5 hour then incubated overnight at 4ºC in 2.5% NFDM in TBS-T containing primary antibodies for rabbit anti-Sox17 1:500 (Abcam) or rabbit anti-LEF-1 1:500 (Cell Signaling Technology). Following primary incubation, blots were washed then incubated in the 2.5% NFDM containing the appropriate horseradish peroxidase-linked secondary (1:5,000; Santa Cruz Biotechnology) for 45 min at room temperature. Clarity ECL substrate (Bio-Rad) and the ChemiDoc MP system (Bio-Rad) were used to visualize immunotagged protein bands. Blots were stripped with stripping buffer (Restore Plus; ThermoScientific) and re-probed with a mouse anti-β-actin (1:2000; Cell Signaling Technology) antibody as a loading control. Densitometry of bands was performed using ImageLab software (Bio-Rad); density values were corrected for loading variations within each blot using the amount of β-actin expression.

Statistics. To detect statistically significant differences in mean values between a control and mutant gentoype at one developmental time point (vessel density, β-gal+ ECs per vessel length, cell proliferation density, qPCR analysis), Student *t*-tests were used. Analysis that compared more than two groups (e.g., control and two mutant gentoypes, multiple developmental time-points, multiple cell culture treatment conditions, etc.), a one-way analysis of variance (ANOVA) with Tukey's post-hoc analysis was used to detect statistically significant differences between genotypes or treatment conditions using pairwise analysis. The standard error of the mean (SEM) is reported on all graphs.

Results

Cerebrovascular development is impaired in *Rdh10* mutant embryos

Mouse mutants with an ENU-induced point mutation in the RA-biosynthetic enzyme *Rdh10* have reduced levels of RA and display developmental defects consistent with RA-deficiency (Ashique et al.,

2012). *Rdh10* mutants survive until E14.5 thus permitting analysis of RA-related neurovascular defects. E14.5 *Rdh10* mutants display severe defects in eye, craniofacial development and as well as significant expansion of the dorsal telencephalon (Fig. 1A). The latter phenotype is caused by expansion of neocortical progenitors at the expense of neuron generation resulting in an elongated, 'ballooned' neocortex (Siegenthaler et al., 2009). In sections at the level of the forebrain, notably fewer (Fig. 1A arrow) or, in some areas, no isolectin-B4+ (Ib4+) blood vessels (Fig. 1A, open arrow) were present in the long, thin neocortex in the *Rdh10* mutant brain. Avascular neocortical regions were not observed consistently though were usually seen in regions where the neocortex was very thin. Higher magnification images of the neocortex revealed fewer, though larger diameter vessels in the notably thinned *Rdh10* mutant neocortex (Fig. 1B, arrow). Numerous large diameter vessels were seen in the PNVP vasculature adjacent to the *Rdh10* mutant neocortex (Fig. 1B, open arrows). In contrast to the neocortical vasculature, Ib4+ vessels in the thalamus of *Rdh10* mutants were not overtly different from control (Fig. 1B), indicating that severe vascular defects may be limited to the neocortex.

Blood vessels in the developing cortex appeared reduced in number while vessels in the PNVP appeared more numerous. Decreased EC proliferation within the neocortex and increased EC proliferation within the PVNP could account for these differences. We examined this possibility by quantifying the percent of GLUT-1+ ECs in the neocortical plexus and PNVP that incorporate the thymidine analog BrdU (EC proliferation index). Significantly more GLUT-1+/BrdU+ ECs were observed in *Rdh10* mutant PNVP overlying the neocortex (Fig. 1C & D) whereas EC proliferation was significantly reduced in the vascular plexus within the *Rdh10* neocortex (Fig. 1C & D). Of note, *Rdh10* mutants expression of GLUT-1, a glucose transporter enriched in CNS ECs whose expression is induced early in the CNS vasculature by WNT signaling (Daneman et al. 2010), appeared decreased in neocortical blood vessels and elevated in the neuroepithelial cells of the VZ as compared to control (Fig. 1C).

We next compared E14.5 cerebrovascular density to E12.5, an earlier time point when neocortical defects in *Rdh10* mutant are not as severe. At E12.5, the thickness of the neocortical wall was comparable in *Rdh10* mutants to littermate control tissue (Fig. 1E & F, left panels) and the vascular density in the neocortex was not significantly different between control and *Rdh10* mutant embryos (Fig. 1G). Of note, however, vessels in the *Rdh10* mutant embryos appeared enlarged at this age (Fig. 1F, open arrows) indicating vascular defects are potentially present at this time point. In control mice both the neocortical wall and vasculature show significant growth between E12.5 and E14.5. However, from E12.5 to E14.5 in *Rdh10* mutants there was substantial lateral expansion but very little radial expansion of the neocortex and blood vessel growth was significantly impaired (Fig. 1E, F & G). We next quantified vascular density in the striatum and thalamus of control and *Rdh10* mutants at both E12.5 and E14.5 and found no differences in vascular growth between *Rdh10* mutant and control samples (Fig. 1G). This analysis demonstrates 1) cerebrovascular defects may emerge early in *Rdh10* mutants during neocortical development and worsen over time and 2) vascular growth defects in *Rdh10* mutants are specific to the neocortical region.

Elevated *Vegfa* expression is associated with an up-regulation of hypoxia-inducible genes in *Rdh10* mutant neocortices and non-neocortical brain regions

Neuroepithelial-derived VEGFA is a major regulator of vascular growth in the CNS (Haigh et al., 2003; Raab et al., 2004; James et al., 2009). Reduced VEGF-A from neural progenitors in the neocortical VZ of *Rdh10* mutants could contribute to aberrant vascular growth in the neocortex. To test this, we quantified *Vegfa* gene expression using RNA isolated from neocortex only or all other non-neocortical brain structures (striatum, thalamus, midbrain, hindbrain) at E13.5. *Vegfa* expression was substantially increased in both the *Rdh10* mutant neocortical and non-neocortical samples as compared to littermate controls (Fig. 2A). *Vegfa* expression is induced in response to hypoxia and therefore the increase in *Vegfa* expression we observe in the *Rdh10* mutants could be due to tissue hypoxia. We tested

this possibility by analyzing the expression of known hypoxia-inducible genes *Ldha*, *Pdk1* and *Cox4i2* (Firth et al., 1994; Kim et al., 2006; Fukuda et al., 2007). All of these hypoxia-inducible genes were also up-regulated (Fig. 2A) indicating the elevated *Vegfa* expression in the neocortex is likely due to tissue hypoxia. Interestingly, increased expression of hypoxia genes were also observed in the non-neocortical regions of the *Rdh10* mutants even though vascular development was not significantly affected in these regions (Fig. 2A). Expression of *Slc2a1*, which encodes the GLUT-1 protein, is also increased by hypoxia through a similar hypoxia inducible factor-mediated mechanism (Chen et al., 2001). We noticed that GLUT-1 appeared up-regulated in the neuroepithelium of *Rdh10* mutant neocortices (Fig. 1C). We found that *Slc2a1* expression was up-regulated in the neocortex but not in the non-neocortex of the *Rdh10* mutants (Fig. 2B). Furthermore, quantification of GLUT-1 immunofluorescent intensity in neocortical VZ and in non-neocortical brain regions (striatum and thalamus) showed that VZ GLUT-1 expression was significantly increased in the *Rdh10* mutant neocortex but not in other brain regions (Fig. 2C). This is evident in low magnification images of E14.5 control and *Rdh10* mutant brains where GLUT-1 expression was limited to blood vessels in the control and in non-neocortical brain regions of *Rdh10* mutants however regions of high neural GLUT-1 expression were observed specifically in the *Rdh10* mutant neocortex (Fig. 2D, arrows and 2E). Collectively this data indicates that *Rdh10* mutants have tissue hypoxia throughout the embryonic brain, possibly due to systemic defects in embryonic development. However, focal upregulation of GLUT-1 in the neocortex suggests hypoxia is more pronounced in the neocortex likely due to impaired vascular growth specifically in this brain structure.

Endothelial WNT signaling is diminished in the *Rdh10* mutant cerebrovasculature and correlates with elevated expression of WNT inhibitors in the neocortex.

WNT signaling in CNS ECs, activated by neural derived WNT ligands WNT7a and WNT7b, is important for vascular growth, stabilization and acquisition of BBB properties. The neocortical vascular growth defects and altered expression of GLUT-1 in the vasculature and neuroepithelium in *Rdh10*

mutants (Figs. 1 and 2) is similar to mutant mice in which WNT7a and WNT7b are both deleted (Stenman et al., 2008) and when the WNT signaling component β-catenin is conditionally deleted from ECs (Daneman et al., 2009; Zhou et al., 2014). Thus, we next looked at the integrity of the WNT pathway (e.g., endothelial WNT signaling, WNT ligands and inhibitors) in *Rdh10* mutant neocortices. We used the WNT signaling reporter mouse line *Bat-gal-lacZ* to assess endothelial WNT signaling in the *Rdh10* mutant neocortical vasculature. β-galactosidase positive (β-gal+) ECs, as determined by co-localization with Ib4, were readily apparent in the control neocortical vasculature (Fig. 3A, arrow) however β-gal+ ECs were nearly absent in the *Rdh10* mutant neocortical vasculature and overlying PNVP (Fig. 3A, right panel). β-gal+ neural cells in the neocortex (Fig. 3A, open arrows) and in the overlying skin mesenchyme (Fig. 3A, double-arrows) were present in *Rdh10* mutants. We quantified the number of β-gal+ ECs per vessel length at E12.5 and E14.5 in the neocortices of control and *Rdh10* mutant embryos. The density of β-gal+ ECs significantly increased across developmental time points in wildtype neocortices but was significantly reduced at both time points in *Rdh10* mutants (Fig. 3B).

We assayed expression of two known targets of WNT-mediated gene transcription in the CNS vasculature, Claudin-3 (Liebner et al., 2008) and LEF-1 (Filali et al., 2002). Consistent with *Bat-gal-LacZ* expression analysis, Claudin-3 (Fig. 3C, D) and LEF-1 (Fig. 3E) expression were appreciably decreased in the neocortical vasculature of *Rdh10* mutants. In conjunction with our quantitative analysis using the WNT signaling reporter, decreased expression of vascular LEF-1 and Claudin-3 in *Rdh10* mutants demonstrates decreased endothelial WNT signaling within the neocortex of these mutants.

We next tested if the expression of WNT7a and WNT7b transcripts were reduced in neocortices of *Rdh10* mutants, however qPCR analysis showed no difference between wild-type and *Rdh10* mutants at E13.5 (Fig. 3F). RA plays a crucial role in the development of the lung primordium by suppressing the expression of the WNT inhibitor Dkk1 (Chen et al., 2010). It is possible that RA inhibits the expression of Dkk1 in the neocortex to ensure proper endothelial WNT signaling occurs. Expression of

Dkk1 as well as certain WNT inhibitors soluble frizzled receptor proteins (sFRPs) (*Sfrp1*, *Sfrp2*, and *Sfrp5*) were significantly upregulated in *Rdh10* mutant neocortices (Fig. 3F). Elevated expression of WNT inhibitors was specific to the neocortex of *Rdh10* mutants since no significant changes in WNT inhibitor expression were observed in non-neocortical regions (Fig. 3F).

Dkk1 and *Sfrp5* were the most robustly upregulated of the WNT inhibitors assayed in the *Rdh10* mutant neocortices and RA has been shown to directly suppress *Dkk1* transcription in other developing organs (Chen et al., 2010). We used cultured neocortical progenitors cells (NPCs) derived from E14 mouse neocortex to test the idea that RA may be required to suppress expression of *Dkk1* and *Sfrp5* in the developing neocortex. Treatment with RA significantly down-regulated expression of *Dkk1* and *Sfrp5* gene expression in NPCs (Fig. 3G). RA-mediated inhibition of *Dkk1* and *Sfrp5* expression was abrogated by the addition of a pan-RAR inhibitor suggesting that RARs are required to mediate the effect of RA on *Sfrp5* and *Dkk1* expression (Fig. 3G). We tested if RA modulated expression of *Dkk1* and *Sfrp5* in cultured cortical neurons however *Dkk1* and *Sfrp5* were undetectable in cultured neurons (data not shown). Collectively this data shows that severe cerebrovascular growth defects in *Rdh10* mutants correlate with diminished endothelial WNT signaling, a pathway required for brain vascular development. Further, our data indicate RA may function in the neocortex to suppress expression WNT inhibitors in neocortical progenitors thus creating a permissive environment for WNT-mediated cerebrovascular growth.

RA functions cell-autonomously in brain ECs to modulate WNT signaling.

Severe vascular growth defects and increased expression of WNT inhibitors was only observed in the *Rdh10* mutant neocortex, indicating a specific **non-cell autonomous** role for RA in this brain structure through regulating WNT inhibitor expression by neocortical progenitors. RARs are expressed by brain ECs, indicating RA signaling is likely active in brain ECs and may have an important, cell-autonomous function in this cell type. Our first indication of this was an observation from our analysis

of endothelial WNT signaling in non-neocortical brain regions of *Rdh10* mutants using endothelial *Bat-gal-lacZ* expression as a readout of WNT activity. In the E14.5 thalamus, β-gal+ ECs were evident in the thalamic vasculature of both *Bat-gal/+* and *Rdh10; Bat-gal/+* mutant samples however the number and intensity of β-gal+ ECs was increased in the *Rdh10* mutant (Fig. 4A, open arrows). Quantification of the number of β-gal+ ECs per vessel length in the striatal and thalamic vasculature at E14.5 revealed a significant increase in β-gal+ ECs in *Rdh10* mutants (β-gal+/Ib4+ cells per 100 µm vessel length - wildtype: 1.8 ± 0.06 SEM vs *Rdh10* mutant: 2.4 ± 0.17 SEM n≥3 p= 0.03). This data shows that endothelial WNT signaling is increased in non-neocortical regions of the *Rdh10* mutant brain.

RA signaling through its receptors has been shown to inhibit WNT signaling in a variety of cell types (Easwaran et al., 1999; Mulholland et al., 2005; Chanda et al., 2013) raising the possibility that RA may directly regulate WNT signaling in brain ECs. To begin to test this idea, we developed a mouse model in which RA signaling is specifically disrupted in brain ECs using an inducible EC-specific CreER^{T2} line (*Pdgfbi-CreER^{T2}*, referred to here as *PdgfbiCre*) (Claxton et al., 2008) and a conditional, dominant negative version of RARα allele located in the *ROSA26R* locus (*dnRAR403-flox*) (Rosselot et al., 2010). DnRARα403 is a truncation mutant of the human RARα that can bind to endogenous RARs but when expressed in a cell disrupts endogenous RA signaling activity (Tsai et al., 1992; Damm et al., 1993). To look at the effect of disrupted endothelial RA signaling on prenatal brain vascular development, pregnant females were injected with tamoxifen at E9 and E10 to induce Cre-mediated expression of dnRARα403 in ECs and fetuses were collected at E14.5, E16.5 and E18.5 (Fig. 4B). To confirm vascular-specific expression of the *PdgfbiCre* transgene in the brain, we took advantage of the IRES-EGFP present in the transgene and used a GFP antibody to detect transgene expression. At E14.5, GFP expression was observed in Ib4+ blood vessels in the brain but was not Ib4+ microglia which could be distinguished by their ramified cell morphology (Fig. 4B). Grossly, E18.5 fetuses expressing one or two copies of the *dnRAR403-flox* allele (*PdgfbiCre; dnRAR403-fl/+* and *PdgfbiCre;*

dnRAR403-fl/fl) had no obvious phenotype (Fig. 4C). In the brain, small hemorrhages were evident in E18.5 cerebral hemispheres in *PdgfbiCre; dnRAR403-fl/fl* animals (Fig. 4D). This was seen as extravasated GLUT-1+ red blood cells in sections (Fig. 4E, open arrows) next to amoeboid-shaped Ib4+ microglia (Fig. 4E, arrow in inset), indicative of activated microglia caused by micro-bleeds. Cerebrovascular density at E18.5 was not overtly affected when RA signaling was disrupted in ECs (Ib4+ vessel length/area of analysis – control (*PdgfbiCre/+* or *dnRAR403-flox)*: 0.35 ± 0.007 vs *PdgfbiCre; dnRAR403-fl/+*: 0.36 ± 0.012 vs *PdgfbiCre; dnRAR403-fl/fl*: 0.37 ± 0.004 n=3, p=0.5). This is consistent with our analysis of non-neocortical vasculature in *Rdh10* mutant embryos and brain vascular development in embryos exposed to RAR inhibitors (Mizee et al., 2013). However, enlarged vessels were evident in the mutant cerebrovasculature (Fig. 4F, arrows) and cerebrovascular vessel diameter was significantly increased in *PdgfbiCre; dnRAR403-fl/fl* mutants at E18.5 (control (*PdgfbiCre/+* or *dnRAR403-flox)*: 5.8 µm ± 0.09 vs *PdgfbiCre; dnRAR403-fl/fl*: 7.0 µm ± 0.232 n=3, p=0.035). This data shows that disrupting RA signaling in brain ECs causes morphological changes in blood vessels and focal vascular instability (e.g., micro-bleeds) but does not appear to alter angiogenic growth.

Possibly, disrupting RA signaling in the vasculature could abrogate neurodevelopmental processes such as neural progenitor proliferation and differentiation. We examined this in the E16.5 neocortex of *PdgfbiCre; dnRAR403-fl* control and mutant animals by looking at expression of established progenitor cell (Pax6 and Tbr2) and post-mitotic neuronal markers (Ctip2). Qualitatively, the Pax6+ and Tbr2+ expressing progenitor populations appeared similar in *PdgfbiCre; dnRAR403-flox* control and mutant mice as did the positioning of Ctip2+ neurons in the lower part of the cortical plate (Fig. 4G). This data indicates that disruption of endothelial RA signaling and any subsequent effects on vascular development and stability (e.g., microbleeds) does not grossly affect corticogenesis.

To directly test if RA signaling functions cell-autonomously in brain ECs to inhibit WNT transcriptional activity, we bred the WNT transcriptional reporter line *Bat-gal-lacZ* into the *PdgfbiCre; dnRAR403-flox* control and mutant background and analyzed EC β-gal expression in the forebrain regions (e.g., neocortex, striatum and thalamus). β-gal+ ECs were more numerous in E18.5 *PdgfbiCre; dnRAR403-fl/fl* fetal brain as compared to control (Fig. 5A, B open arrows) indicating that endothelial WNT signaling is more active when endothelial RA signaling is disrupted. Quantification of β-gal+ ECs per vessel lengths showed a significant increase in *PdgfbiCre; dnRAR403-fl/+* and even more so in *PdgfbiCre; dnRAR403-fl/fl* mutants (Fig, 5C). Expression of LEF-1, a direct transcriptional target of WNT signaling expressed by brain ECs, appeared elevated in *PdgfbiCre; dnRAR403-fl/fl* mutants as compared to control (Fig. 5D, E) and quantification of LEF-1 protein expression in cortical lysate showed a significant increase in *PdgfbiCre; dnRAR403-fl/fl* mutant samples (LEF-1 band density relative to β-actin - *PdgfbiCre/+ or dnRAR403-flox*: 0.85 ± 0.09 vs *PdgfbiCre; dnRAR403-fl/fl*: 1.4 ± 0.2 p=0.046 n=4). We looked at expression of LEF-1 in the head vasculature of control and *PdgfbiCre; dnRAR403-fl/fl* mutant to see if disrupted RA signaling in non-CNS vessels leads to ectopic WNT activity. LEF-1 was expressed strongly expressed in the skin but was not detectable in Ib4+ blood vessels in either genotype (Fig. 5G, arrows). This indicates that the interaction between RA and WNT signaling in ECs is likely limited to the brain vasculature. Further, this shows that expression of the *dnRAR403-flox* allele alone does not activate endothelial WNT signaling. Collectively our analysis of non-cortical vasculature in *Rdh10* mutants and *Pdgfbi-Cre; dnRAR403-flox* mutants demonstrates that disruption of RA signaling in brain ECs causes increased WNT signaling and points to a novel, cell-autonomous function for RA as an inhibitor of endothelial WNT signaling in the developing brain.

RA exposure inhibits endothelial WNT signaling both *in vivo* and in cultured ECs.

We next tested if RA is sufficient to inhibit WNT activity in brain ECs by feeding pregnant *Bat-gal-lacZ/+* mice a RA-enriched diet from E10 to E14.5 or E16.5 and then analyzing β-gal+ EC density in the neocortical vasculature (Fig. 6A). Exposure to RA did not significantly alter β-gal+ endothelial cell density at E14.5 (Fig. 6B). Between E14.5 and E16.5 there was a significant increase in the β-gal+ EC density in fetuses from control diet females but this was not observed in RA-exposed animals, resulting in a significant difference between control and RA-diet at E16.5 (Fig. 6B). The RA-dependent reduction in WNT signaling did not affect neocortical vascular density at either age (Fig. 6C), indicating that the alterations in RA and WNT signaling caused by exogenous RA exposure did not overtly impact neurovascular growth.

Our *in vivo* data points to an inhibitory effect of RA on WNT signaling but it is not clear if it can block WNT-mediated effects on brain EC behavior. We tested this in culture by determining whether RA inhibits the effect of WNT ligands on brain EC migration and proliferation. Treatment with the WNT ligand WNT7a promotes transwell migration of the mouse brain endothelioma cell line bEnd.3 (Daneman et al., 2009) and we observed the same effect with WNT3a (Fig. 6D) and Wnt7a. RA in the nanomolar range had no effect on bEnd.3 cell transwell migration but blocked the pro-migratory effect of WNT3a (Fig. 6D) and WNT7a on migration (# of cells per 10 field: control: 963 ± 112 SEM; RA (50 nM): 1070 ±146 SEM; WNT7a (5ug/ml): 1256 ± 37 SEM; RA+WNT7a: 945 ± 72 SEM; control vs WNT7a: p=0.0062; WNT7a vs RA+WNT7a: p=0.0027; n=3). The same concentration of WNT3a inhibited bEnd.3 cell proliferation, an effect that was blocked when cells were co-treated with RA (Fig. 6E). This data further confirms that RA can directly regulate endothelial WNT signaling and shows that RA can modulate WNT mediated endothelial cell behavior

We next sought to determine whether the effect of RA on WNT signaling was at the level of RARs. We tested RARα specifically as it was the most abundant RAR expressed by fetal brain microvessels, which contain ECs (Fig. 6F). To do this we manipulated RA signaling in cultured cells

expressing a WNT-β-catenin signaling reporter. HEK293 cells were transfected with TOP-Flash (containing 7 copies of the TCF/LEF binding site upstream of a firefly luciferase gene) or FOP-Flash (containing 7 mutated copies of the TCF/LEF binding site upstream of a firefly luciferase gene). Activation of WNT signaling induces accumulation and subsequent translocation of β-catenin to the nucleus, which interacts with TCF/LEF transcription factors activating the TOP-Flash reporter construct but not the FOP-Flash reporter construct. Cells were co-transfected with control (pCIG), RARα, or RXRβ expression vectors. Cells transfected with control vector and treated with WNT3a showed enhanced TOP-Flash activity over FOP-Flash activity ($p<0.001$), whereas treatment with RA only had no significant effect on reporter activity with control vector (Fig. 6G). Co-treatment of WNT3a and RA to cells transfected with control vector led to reduced activation of the TOP-flash reporter as compared to WNT3a alone (Fig. 6G). Co-transfection of RARα had a significant, inhibitory effect on WNT signaling and decreased TOP-Flash activation by 70.6% following WNT3a treatment ($p<0.001$), by 81.1% following RA treatment ($p<0.001$), and by 90.2% following co-treatment with WNT3a and RA ($p<0.001$) compared to vector controls (Fig. 6G). Interestingly, co-transfection of another retinoid receptor, RXRβ, did not alter WNT signaling activation following WNT3a, RA or combined WNT3a and RA treatment compared to similar treated vector controls (Fig. 6H). These results show that RARα can regulate WNT transcriptional activity.

We next sought to determine whether disruption of RA signaling in cells altered their responsiveness to WNT ligands. To do this, cells were co-transfected with the same dominant-negative RARα construct (dnRARα403) used to construct the *dnRAR403-flox* allele used in our *in vivo* experiments (Damm et al., 1993; Sen et al., 2005). Expression of this truncated construct interferes with endogenous RA signaling because the transcriptional regulatory domain of the receptor is deleted (Damm et al., 1993; Sen et al., 2005; Rajaii et al., 2008). Expression of the dnRARα403 construct in

cells without treatment of WNT3a or RA had no effect on TOP flash reporter activity (Fig. 6I) showing that expression of dominant negative receptor does not directly activate WNT transcriptional activity. In cells expressing the dnRARα403 construct, WNT3a-mediated activation of the TOP-Flash reporter was substantially increased as compared to the WNT3a treated cells with control vector (Fig. 6I). This shows that expression of dnRARα403 disrupts the normal RAR-mediated inhibition of WNT signaling within cells, possibly by displacing endogenous receptors in retinoid receptor complexes. We observed an RA-dependent component as co-treatment with RA and WNT3a dampened the activation effect of dnRARα (Fig. 6I). Previous studies have shown that dnRARα403 can still bind RA ligand, although with less affinity than wild type RARα (Damm et al., 1993). Together, these studies confirm a reciprocal relationship between WNT and RA signaling at the level of RARs.

Sox17 is a target of WNT signaling in fetal brain ECs and is up-regulated following disruption of RA signaling

WNT signaling regulates neurovascular development in the CNS and our evidence points to RA signaling as a modulator of WNT signaling in brain ECs. Sox17 is a transcription factor that is required for vascular development and its expression is regulated by endothelial WNT signaling in the post-natal CNS vasculature (Ye et al., 2009; Corada et al., 2013). We tested if the latter was also the case for the fetal brain vasculature using mice with EC conditional knockdown of WNT signaling component β-catenin (*PdgfbiCre; Ctnnb1-flox*). At E14.5, Sox17 was expressed, to varying to degrees, by ECs in the neocortex whereas Sox17 expression was appreciable decreased in dysplastic blood vessels of *PdgfbiCre; Ctnnb1-fl/fl* mutants (Fig. 7A). Moreover, *Sox17*, along with WNT transcriptional targets *Lef1* and *Axin2*, expression was significantly reduced in the fetal brain microvasculature isolated from E18.5 *PdgfbiCre; Ctnnb1-fl/fl* mutant brains (Fig. 7B). This data shows that Sox17 is regulated by WNT-β-catenin signaling in the fetal brain vasculature.

We next investigated Sox17 in the context of disrupted RA signaling using *PdgfbiCre; dnRAR403-fl/fl* mutants that have elevated endothelial WNT transcriptional activity. High expression of Sox17 was observed in some vessels in the E18.5 control cortex (Fig. 7C, arrows in left panel) whereas other vessels had low Sox17 expression (Fig. 7C, open arrows in left panel). In contrast, Sox17 was strongly expressed by all blood vessels in the *PdgfbiCre; dnRAR403-fl/fl* fetal neocortex (Fig. 7C, arrows in right panel) and Sox17 protein expression, quantified via immunoblot, was significantly elevated in fetal cortical lysate as compared to control (Fig. 7D; Sox17 band density relative to β-actin - *PdgfbiCre/+ or dnRAR403-flox*: 1.3 ± 0.07 vs *PDGFBiCre; dnRAR403-fl/fl*: 1.8 ± 0.14 p=0.019 n=4). These data show that brain ECs with disrupted RA signaling, and increased WNT signaling, have increased Sox17 expression.

Sox17 is expressed by arterial ECs and is required for expression of artery specific markers (Corada et al., 2013). In the fetal brain vasculature, we found Sox17 was weakly expressed by venous blood vessels, identified by nuclear receptor Coup-TFII (Fig. 8A, open arrows). Sox17 was highly expressed by CoupTFII-negative vessels (Fig. 8A, arrow) and arterial vessels identified by *Ephrin-B2-GFP* in the EC nuclei (Fig. 8C, arrow). Expression of Sox17 was appreciable higher in Coup-TFII+ venous ECs in *PdgfbiCre; dnRAR403-fl/fl* fetal brains as compared to control brain vasculature (Fig. 8B, open arrows). Coup-TFII was also expressed by perivascular mural cells (Fig. 8A, B, double-arrow) and some neurons (Fig. 8B, triple-arrow). High expression of Sox17 was limited to *Ephrin B2-GFP*+ vessels in control brain whereas high Sox17 was observed in both *Ephrin B2-GFP*+ and *Ephrin-B2-GFP*- ECs in *PdgfbiCre; dnRAR403-fl/fl* fetal brain vasculature (Fig. 8C and D, arrows: *Ephrin-B2-GFP*+/Sox17+, open arrows: *Ephrin-B2-GFP*-/Sox17+). GFP signal was visible in EC membrane in *PdgfbiCre; dnRAR403-fl/fl* sections but not control due to IRES-GFP present in *PdgfbiCre* allele (Fig. 8D, triple-arrow). The increase in Sox17 in the vasculature, including venous blood vessels that normally have low levels of Sox17, in *PdgfbiCre; dnRAR403-fl/fl* fetal brains did not result in defects in arterial-venous

specification. This is based on the observation that mutants retained expression of venous marker Coup-TFII and had both *Ephrin-B2-GFP* positive and negative vessels (Fig. 8B, D). Collectively our data suggests that RA signaling in endothelial cells may act as a balance to ensure normal WNT-driven brain vascular development and moderate endothelial Sox17 expression levels.

Discussion (1500 words)

Here we demonstrate that RA has separate functions during brain vascular development. **In the developing neocortex, RA functions non-cell autonomously to promote endothelial WNT signaling and cerebrovascular growth via a mechanism that involves suppressing expression of WNT inhibitors by neocortical progenitors and possibly neurons** (Fig. 9A). RA also functions cell-autonomously in brain ECs to inhibit endothelial WNT signaling and prevent ectopic expression of WNT target genes like Sox17 (Fig. 9B). Our work, for the first time, places a factor upstream of WNT pathway in brain vascular development and reveals a multi-faceted mechanism through which RA acts on both neural and vascular cells to target endothelial WNT signaling activity.

Rdh10 mutants globally lack RA and have significant developmental defects consistent with RA-deficiency. Here we show that, in addition to the defects in neocortical development, growth of the cerebrovasculature is severely impaired in *Rdh10* mutants. Other brain regions have relatively normal vasculature pointing to a unique role for RA in cerebrovascular development. We provide data that two major neuro-angiogenic pathways, VEGFA and WNT, are disrupted in *Rdh10* mutant neocortices. With regard to VEGFA, we see that *Vegfa* and several other hypoxia-inducible genes are upregulated in both the *Rdh10* mutant neocortex and non-neocortical brain regions. This data indicates widespread hypoxia in the developing brain, possibly caused by other developmental defects in *Rdh10* mutants. Tissue hypoxia appears to be more pronounced in the *Rdh10* mutant neocortex, as evidenced by selective neural upregulation of GLUT-1 in this brain region, possibly due to severe cerebrovascular growth defects. Despite elevated *Vegfa* gene expression, we do not observe vascular overgrowth and impaired vascular

integrity (e.g., hemorrhage) in the *Rdh10* mutant brain, two features that have been reported in mutant mice with conditional upregulation of *Vegfa* in the neuroepithelium (Yang et al., 2013). Possibly, tissue hypoxia and *Vegfa* upregulation only begin to emerge at the end of *Rdh10* mutant viability (E14.5) and therefore VEGF-A protein levels are only elevated at late time points. At earlier developmental time points (E12.5), VEGF-A could be decreased in the *Rdh10* mutant neocortex and possibly contribute to defects in cerebrovascular development, namely enlarged vasculature, seen at these time points. Our analysis does not differentiate between *Vegfa* transcript expressed by different cell types present in the tissue samples. VEGF-A is expressed by neural progenitors where it is required for vascular growth in the brain however VEGF-A expressed by ECs is reported to be required for neocortical and vascular development (Li et al., 2013). Increased VEGF-A from different cell sources in the neocortex could differentially effect vascular and neocortical development however more studies are needed to address this specifically.

Perhaps more compelling is our evidence demonstrating near absence of endothelial WNT signaling concurrent with cerebrovascular defects in *Rdh10* mutants. Endothelial WNT signaling, stimulated by WNT7a and WNT7b produced by progenitors and neurons in the developing brain, is required for brain vascular growth, stability and BBB formation (Stenman et al., 2008; Daneman et al., 2009; Zhou et al., 2014). Therefore reduced endothelial WNT signaling is likely a major factor contributing to defective cerebrovascular development in *Rdh10* mutants. We provide evidence of a **non-cell autonomous function for RA** as the underlying cause of reduced endothelial WNT signaling in *Rdh10* mutants. We show that WNT inhibitors Dkk1 and several sFRPs are specifically upregulated in the *Rdh10* mutant neocortex but no other brain regions. Dkk1 is a potent inhibitor of canonical WNT signaling through direct binding to WNT co-receptors low-density lipoprotein receptor-related 5 and 6 (LRP5/6) whereas sFRPs antagonize WNT signaling by interfering with the interaction between WNT ligands and receptors (Mao et al., 2001). Dkk1 and sFRP5 show the most substantial increase in gene

expression in the *Rdh10* neocortex and we provide cell culture data that RA, functioning through RARs, is sufficient to suppress *Dkk1* and *Sfrp5* gene expression in **neocortical progenitors**. This sets up a model in which RA-deficiency in *Rdh10* mutants leads to loss of RA-mediated suppression WNT inhibitors in neocortical progenitors, **and possibly post-mitotic neurons**, and the resulting ectopic expression of WNT inhibitors causes impairment of endothelial WNT signaling in the neocortex (Fig. 9A). Equally important to consider is that the cerebrovascular defects and diminished endothelial WNT signaling are occurring within a severely dysplastic neocortex caused by lack of RA. Reduced numbers of neocortical progenitors and neurons caused by aberrant proliferation and differentiation likely plays some role in altered expression of WNT pathway proteins. This is indicated by analysis showing that vascular growth defects are most pronounced at E14.5, a time point when the proliferative and post-mitotic regions of the *Rdh10* mutant neocortex are substantially thinner than control animals. An intriguing possibility is that persistent tissue hypoxia in the neocortex could be contributing to the aberrant progenitor proliferation and differentiation in the *Rdh10* mutant cortex. In this way, the vascular defects could be a major contributor or, at least, exacerbating defects in corticogenesis. Recent work demonstrated that the neocortical progenitors switch from self-renewing divisions to neuro-generating divisions coincided with cerebrovascular growth and reduced levels of tissue hypoxia (Lange et al., 2016). Further studies are needed to understand how defective corticogenesis and impaired cerebrovascular development are connected in *Rdh10* mutant animals.

In the non-neocortical brain regions of *Rdh10* mutants, we found that endothelial WNT signaling was elevated. This was our first indication that RA may function cell-autonomously in brain ECs to inhibit WNT signaling. This observation was supported by increased endothelial WNT signaling in mutants with EC-specific disruption of RA signaling and data showing that exposure of embryos to excess RA diminishes brain endothelial WNT signaling. It is important to note that analysis of endothelial WNT signaling in *PdgfbiCre; dnRAR403-flox* mutants and RA-treated embryos

encompassed neocortical and non-neocortical (striatum, thalamus) structures. This suggests that the cell-autonomous function for RA signaling in brain ECs throughout the brain is to inhibit endothelial WNT signaling. **In the neocortex, however, our data demonstrates RA has a separate, non-cell autonomous function with regard to endothelial WNT signaling: controlling expression of WNT inhibitors to create a permissive environment for WNT-mediated cerebrovascular growth. Presumably, loss of RA in the neocortex of *Rdh10* mutants lessens the inhibitory effect of RA signaling on endothelial WNT transcriptional activity. This is observed in other *Rdh10* mutant brain regions. However, the substantial increase in WNT inhibitors resulting from loss of RA acting on other cell types likely severely impairs activation of endothelial WNT pathways by WNT ligands. The significance of RA having non-cell and cell-autonomous functions with regard to endothelial WNT signaling specifically in the neocortex is not clear but will be addressed in future studies.**

In the developing CNS, nascent vessels are surrounded by WNT ligands from neural sources. These signals ensure vessel integrity, help initiate and maintain barrier properties in the neurovasculature, features that are required by all CNS ECs (Liebner et al., 2008; Stenman et al., 2008; Daneman et al., 2009; Zhou et al., 2014). Why, then, is RA acting as an inhibitor to this key pathway in brain ECs? Ectopic WNT signaling in the developing embryonic vasculature leads to widespread arterialization (Corada et al., 2010) thus RA might act as an important “brake” on WNT signaling in the neurovasculature to prevent inappropriate acquisition of arterial traits. We do not, however, find evidence of arterialization of brain vessels in *PdgfbiCre; dnRAR403-flox* mutants. Possibly, fetal brain ECs do not respond to elevated WNT signaling in the same way as newly specified ECs. In support of this, when an inducible Cre line was used to express constitutively active β-catenin in ECs after E9.5 the authors did not observe widespread arterialization of the embryonic vasculature (Corada et al., 2010). We hypothesize that RA modulates WNT signaling through its receptor RARα to prevent over-

expression of its target Sox17 (Fig. 9B). Forcing expression of Sox17 in ECs causes defects in brain and retinal vascular development, most notably increased vascular growth (Lee et al., 2014). Of note, we find dysplastic vessels and micro-bleeds in *PdgfbiCre; dnRAR403-flox* mutants that have ectopic Sox17 expression. Forthcoming experiments will address if the micro-bleeds and increased vascular diameter in *PdgfbiCre; dnRAR403-flox* mutants is caused by elevated Sox17 expression and explore the transcriptional targets of Sox17 in brain ECs that mediates its function in the brain endothelium.

Our data showing repression of WNT signaling by RA in CNS ECs is consistent with the established literature on cross-talk between RA and WNT pathways both in development and disease. RA inhibits WNT signaling during hematopoietic stem cell development (Chanda et al., 2013) and in a variety of cancer cell lines with oncogenic β-catenin activity (Mulholland et al., 2005). Modulation of WNT signaling by RA signaling likely occurs at the level of RARα which we show is the main RAR expressed brain fetal brain ECs. RARs can interact with components of the WNT transcriptional complex which includes β-catenin, TCF members and Lef1 and through these interactions modulate WNT-mediated transcription (Easwaran et al., 1999; Shah et al., 2003). Future work looking at the direct interactions between proteins in these two pathways will provide insight into how brain ECs appropriately integrates RA and WNT signaling during brain vascular development.

References

Al Tanoury Z, Piskunov A, Rochette-Egly C (2013) Vitamin A and retinoid signaling: genomic and nongenomic effects. J Lipid Res 54:1761-1775.

Ashique AM, May SR, Kane MA, Folias AE, Phamluong K, Choe Y, Napoli JL, Peterson AS (2012) Morphological defects in a novel Rdh10 mutant that has reduced retinoic acid biosynthesis and signaling. Genesis 50:415-423.

Bauer H, Bauer H, Lametschwandtner A, Amberger A, Ruiz P, Steiner M (1993) Neovascularization and the appearance of morphological characteristics of the blood-brain barrier in the embryonic mouse central nervous system. Brain Res Dev Brain Res 75:269-278.

Bohnsack BL, Lai L, Dolle P, Hirschi KK (2004) Signaling hierarchy downstream of retinoic acid that independently regulates vascular remodeling and endothelial cell proliferation. Genes Dev 18:1345-1358.

Brault V, Moore R, Kutsch S, Ishibashi M, Rowitch DH, McMahon AP, Sommer L, Boussadia O, Kemler R (2001) Inactivation of the beta-catenin gene by Wnt1-Cre-mediated deletion results in dramatic brain malformation and failure of craniofacial development. Development 128:1253-1264.

Breier G, Albrecht U, Sterrer S, Risau W (1992) Expression of vascular endothelial growth factor during embryonic angiogenesis and endothelial cell differentiation. Development 114:521-532.

Chanda B, Ditadi A, Iscove NN, Keller G (2013) Retinoic acid signaling is essential for embryonic hematopoietic stem cell development. Cell 155:215-227.

Chen C, Pore N, Behrooz A, Ismail-Beigi F, Maity A (2001) Regulation of glut1 mRNA by hypoxia-inducible factor-1. Interaction between H-ras and hypoxia. J Biol Chem 276:9519-9525.

Chen F, Cao Y, Qian J, Shao F, Niederreither K, Cardoso WV (2010) A retinoic acid–dependent network in the foregut controls formation of the mouse lung primordium. The Journal of Clinical Investigation 120:2040-2048.

Claxton S, Kostourou V, Jadeja S, Chambon P, Hodivala-Dilke K, Fruttiger M (2008) Efficient, inducible Cre-recombinase activation in vascular endothelium. Genesis 46:74-80.

Corada M, Nyqvist D, Orsenigo F, Caprini A, Giampietro C, Taketo MM, Iruela-Arispe ML, Adams RH, Dejana E (2010) The Wnt/beta-catenin pathway modulates vascular remodeling and specification by upregulating Dll4/Notch signaling. Dev Cell 18:938-949.

Corada M, Orsenigo F, Morini MF, Pitulescu ME, Bhat G, Nyqvist D, Breviario F, Conti V, Briot A, Iruela-Arispe ML, Adams RH, Dejana E (2013) Sox17 is indispensable for acquisition and maintenance of arterial identity. Nat Commun 4:2609.

Damm K, Heyman RA, Umesono K, Evans RM (1993) Functional inhibition of retinoic acid response by dominant negative retinoic acid receptor mutants. Proc Natl Acad Sci U S A 90:2989-2993.

Daneman R, Zhou L, Kebede AA, Barres BA (2010) Pericytes are required for blood-brain barrier integrity during embryogenesis. Nature 468:562-566.

Daneman R, Agalliu D, Zhou L, Kuhnert F, Kuo C, Barres B (2009) Wnt/beta-catenin signaling is required for CNS, but not non-CNS, angiogenesis. Proc Natl Acad Sci U S A 106:641-646.

Easwaran V, Pishvaian M, Salimuddin, Byers S (1999) Cross-regulation of beta-catenin-LEF/TCF and retinoid signaling pathways. Curr Biol 9:1415-1418.

Filali M, Cheng N, Abbott D, Leontiev V, Engelhardt JF (2002) Wnt-3A/beta-catenin signaling induces transcription from the LEF-1 promoter. J Biol Chem 277:33398-33410.

Firth JD, Ebert BL, Pugh CW, Ratcliffe PJ (1994) Oxygen-regulated control elements in the phosphoglycerate kinase 1 and lactate dehydrogenase A genes: similarities with the erythropoietin 3' enhancer. Proc Natl Acad Sci U S A 91:6496-6500.

Fukuda R, Zhang H, Kim JW, Shimoda L, Dang CV, Semenza GL (2007) HIF-1 regulates cytochrome oxidase subunits to optimize efficiency of respiration in hypoxic cells. Cell 129:111-122.

Haigh J, Morelli P, Gerhardt H, Haigh K, Tsien J, Damert A, Miquerol L, Muhlner U, Klein R, Ferrara N, Wagner E, Betsholtz C, Nagy A (2003) Cortical and retinal defects caused by dosage-dependent reductions in VEGF-A paracrine signaling. Dev Biol 262:225-241.

James J, Gewolb C, Bautch V (2009) Neurovascular development uses VEGF-A signaling to regulate blood vessel ingression into the neural tube. Development 136:833-841.

Kim JW, Tchernyshyov I, Semenza GL, Dang CV (2006) HIF-1-mediated expression of pyruvate dehydrogenase kinase: a metabolic switch required for cellular adaptation to hypoxia. Cell Metab 3:177-185.

Lai L, Bohnsack BL, Niederreither K, Hirschi KK (2003) Retinoic acid regulates endothelial cell proliferation during vasculogenesis. Development 130:6465-6474.

Lange C, Turrero Garcia M, Decimo I, Bifari F, Eelen G, Quaegebeur A, Boon R, Zhao H, Boeckx B, Chang J, Wu C, Le Noble F, Lambrechts D, Dewerchin M, Kuo CJ, Huttner WB, Carmeliet P (2016) Relief of hypoxia by angiogenesis promotes neural stem cell differentiation by targeting glycolysis. EMBO J.

Lee SH, Lee S, Yang H, Song S, Kim K, Saunders TL, Yoon JK, Koh GY, Kim I (2014) Notch pathway targets proangiogenic regulator sox17 to restrict angiogenesis. Circ Res 115:215-226.

Li H, Wagner E, McCaffery P, Smith D, Andreadis A, Drager UC (2000) A retinoic acid synthesizing enzyme in ventral retina and telencephalon of the embryonic mouse. Mech Dev 95:283-289.

Li S, Haigh K, Haigh JJ, Vasudevan A (2013) Endothelial VEGF sculpts cortical cytoarchitecture. J Neurosci 33:14809-14815.

Liebner S, Corada M, Bangsow T, Babbage J, Taddei A, Czupalla C, Reis M, Felici A, Wolburg H, Fruttiger M, Taketo M, von Melchner H, Plate K, Gerhardt H, Dejana E (2008) Wnt/beta-catenin signaling controls development of the blood-brain barrier. J Cell Biol 183:409-417.

Lippmann ES, Al-Ahmad A, Azarin SM, Palecek SP, Shusta EV (2014) A retinoic acid-enhanced, multicellular human blood-brain barrier model derived from stem cell sources. Sci Rep 4:4160.

Lohnes D, Mark M, Mendelsohn C, Dolle P, Dierich A, Gorry P, Gansmuller A, Chambon P (1994) Function of the retinoic acid receptors (RARs) during development (I). Craniofacial and skeletal abnormalities in RAR double mutants. Development 120:2723-2748.

Maden M (2001) Role and distribution of retinoic acid during CNS development. Int Rev Cytol 209:1-77.

Mao B, Wu W, Li Y, Hoppe D, Stannek P, Glinka A, Niehrs C (2001) LDL-receptor-related protein 6 is a receptor for Dickkopf proteins. Nature 411:321-325.

Maretto S, Cordenonsi M, Dupont S, Braghetta P, Broccoli V, Hassan AB, Volpin D, Bressan GM, Piccolo S (2003) Mapping Wnt/beta-catenin signaling during mouse development and in colorectal tumors. Proc Natl Acad Sci U S A 100:3299-3304.

Mizee MR, Wooldrik D, Lakeman KA, van Het Hof B, Drexhage JA, Geerts D, Bugiani M, Aronica E, Mebius RE, Prat A, de Vries HE, Reijerkerk A (2013) Retinoic Acid Induces Blood-Brain Barrier Development. J Neurosci 33:1660-1671.

Mulholland DJ, Dedhar S, Coetzee GA, Nelson CC (2005) Interaction of nuclear receptors with the Wnt/beta-catenin/Tcf signaling axis: Wnt you like to know? Endocr Rev 26:898-915.

Nakao T, Ishizawa A, Ogawa R (1988) Observations of vascularization in the spinal cord of mouse embryos, with special reference to development of boundary membranes and perivascular spaces. Anat Rec 221:663-677.

Napoli JL (1999) Retinoic acid: its biosynthesis and metabolism. Prog Nucleic Acid Res Mol Biol 63:139-188.

Raab S, Beck H, Gaumann A, Yüce A, Gerber H, Plate K, Hammes H, Ferrara N, Breier G (2004) Impaired brain angiogenesis and neuronal apoptosis induced by conditional homozygous inactivation of vascular endothelial growth factor. Thromb Haemost 91:595-605.

Rajaii F, Bitzer ZT, Xu Q, Sockanathan S (2008) Expression of the dominant negative retinoid receptor, RAR403, alters telencephalic progenitor proliferation, survival, and cell fate specification. Dev Biol 316:371-382.

Rosselot C, Spraggon L, Chia I, Batourina E, Riccio P, Lu B, Niederreither K, Dolle P, Duester G, Chambon P, Costantini F, Gilbert T, Molotkov A, Mendelsohn C (2010) Non-cell-autonomous retinoid signaling is crucial for renal development. Development 137:283-292.

Schneider RA, Hu D, Rubenstein JL, Maden M, Helms JA (2001) Local retinoid signaling coordinates forebrain and facial morphogenesis by maintaining FGF8 and SHH. Development 128:2755-2767.

Sen J, Harpavat S, Peters MA, Cepko CL (2005) Retinoic acid regulates the expression of dorsoventral topographic guidance molecules in the chick retina. Development 132:5147-5159.

Shah S, Hecht A, Pestell R, Byers SW (2003) Trans-repression of beta-catenin activity by nuclear receptors. J Biol Chem 278:48137-48145.

Shih SC, Smith LE (2005) Quantitative multi-gene transcriptional profiling using real-time PCR with a master template. Exp Mol Pathol 79:14-22.

Siegenthaler J, Choe Y, Patterson K, Hsieh I, Li D, Jaminet S, Daneman R, Kume T, Huang E, Pleasure S (2013) Foxc1 is required by pericytes during fetal brain angiogenesis. In. Biology Open: The Company of Biologists.

Siegenthaler J, Ashique A, Zarbalis K, Patterson K, Hecht J, Kane M, Folias A, Choe Y, May S, Kume T, Napoli J, Peterson A, Pleasure S (2009) Retinoic acid from the meninges regulates cortical neuron generation. Cell 139:597-609.

Smith D, Wagner E, Koul O, McCaffery P, Drager UC (2001) Retinoic acid synthesis for the developing telencephalon. Cereb Cortex 11:894-905.

Stenman J, Rajagopal J, Carroll T, Ishibashi M, McMahon J, McMahon A (2008) Canonical Wnt signaling regulates organ-specific assembly and differentiation of CNS vasculature. Science 322:1247-1250.

Toresson H, Mata de Urquiza A, Fagerstrom C, Perlmann T, Campbell K (1999) Retinoids are produced by glia in the lateral ganglionic eminence and regulate striatal neuron differentiation. Development 126:1317-1326.

Tsai S, Bartelmez S, Heyman R, Damm K, Evans R, Collins SJ (1992) A mutated retinoic acid receptor-alpha exhibiting dominant-negative activity alters the lineage development of a multipotent hematopoietic cell line. Genes Dev 6:2258-2269.

Yang D, Baumann JM, Sun YY, Tang M, Dunn RS, Akeson AL, Kernie SG, Kallapur S, Lindquist DM, Huang EJ, Potter SS, Liang HC, Kuan CY (2013) Overexpression of vascular endothelial growth factor in the germinal matrix induces neurovascular proteases and intraventricular hemorrhage. Sci Transl Med 5:193ra190.

Ye X, Wang Y, Cahill H, Yu M, Badea TC, Smallwood PM, Peachey NS, Nathans J (2009) Norrin, frizzled-4, and Lrp5 signaling in endothelial cells controls a genetic program for retinal vascularization. Cell 139:285-298.

Zarbalis K, Siegenthaler JA, Choe Y, May SR, Peterson AS, Pleasure SJ (2007) Cortical dysplasia and skull defects in mice with a Foxc1 allele reveal the role of meningeal differentiation in regulating cortical development. Proc Natl Acad Sci U S A 104:14002-14007.

Zhang J, Smith D, Yamamoto M, Ma L, McCaffery P (2003) The meninges is a source of retinoic acid for the late-developing hindbrain. J Neurosci 23:7610-7620.

Zhou Y, Wang Y, Tischfield M, Williams J, Smallwood PM, Rattner A, Taketo MM, Nathans J (2014) Canonical WNT signaling components in vascular development and barrier formation. J Clin Invest 124:3825-3846.

Figure 1. Neocortical vascular development in E14.5 *Rdh10* mutant embryos

(A) Ib4-labeled blood vessels in E14.5 wildtype and *Rdh10* mutant forebrain. Open arrow indicates avascular area of the neocortex, arrow indicates reduced vascular plexus in expanded neocortex. (B) High magnification images of E14.5 vascular plexus in the neocortex and thalamus of wildtype and *Rdh10* mutants. Open arrows and arrows indicate enlarged, dysplastic vessels in PNVP and within the neocortex, respectively. (C) Representative images of GLUT-1/BrdU labeling in the two vascular plexus in the neocortex (NC): the superficial perineural vascular plexus (PNVP) and plexus within the neocortex. Open arrows indicate BrdU+/Glut+ cells in both panels. (D) Graphs depicting quantification of endothelial cell (EC) proliferation index in the NC PNVP and NC plexus in E14.5 wildtype and *Rdh10* mutants. Asterisks indicate significance from wildtype value. (E) Low magnification images of E12.5 and E14.5 wildtype and *Rdh10* mutant forebrains. (F) High magnification images of neocortical PNVP and internal vascular plexus at E12.5 and E14.5 in wildtype and *Rdh10* mutants. (G) Graph depicting vascular density in the two genotypes in the neocortex and thalamus at E12.5 and E14.5. Asterisks indicate significance from E12.5 value of the same genotype, # indicates significance from E14.5 wildtype value. Scale bars: (A and E) 500 µm and (B and C) 100 µm.

Figure 2 - Hypoxia inducible targets VEGFA and GLUT-1 are elevated in *Rdh10* mutant neocortices.

(A) Quantitative PCR for hypoxia inducible genes *Vegfa, Ldha, Pdk, and Cox4i2* transcript expression in control and *Rdh10* mutant neocortices and non-neocortical brain structures. (B) Quantitative PCR for *Slc2a1* (GLUT-1) transporter transcript expression in control and *Rdh10* mutant neocortices and non-neocortical brain structures. (C) Quantification of average intensity signal for GLUT-1 in the VZ of neocortical and striatum/thalamus brain regions of control (wildtype, *Rdh10* heterozygous) and *Rdh10* mutants. (D) Low magnification images of GLUT-1 labeling in E14.5 wildtype and *Rdh10* mutant brains at the level of the cortex and striatum. Arrows indicate regions of high neuroepithelial GLUT-1 signal in the *Rdh10* mutant neocortical VZ. (E) High-magnification images of GLUT-1 labeling in the neocortical

VZ and striatum of wildtype and *Rdh10* mutants. Asterisks indicate significance from control ($p<0.05$). Scale bars are 500 µm.

Figure 3. Diminished WNT signaling in *Rdh10* mutant cerebrovasculature

(A) β-galactosidase (β-gal, green) and Ib4 (red) co-immunolabeling in neocortical blood vessels at E14.5 of *Bat-gal-LacZ/+* and *Rdh10* mutant*; Bat-gal-LacZ/+* animals. Arrows indicate β-gal+ ECs, open arrows indicate β-gal+ neural cells, double-head arrows point to β-gal+ cells in the skin. (B) Quantification of number of β-gal+ ECs per vessel length in in the neocortex of control (wildtype and *Rdh10* heterozygous) and *Rdh10* mutant animals at E12.5 and E14.5. Asterisks indicate significance between control at E12.5 and E14.5, # indicates significance from E12.5 wildtype and *# indicates significance from E14.5 wildtype. (C, D) Arrows indicate Ib4+ (red) vessels with Claudin-3 (green) signal in the neocortical region of a control, *Bat-gal/+* brain. Open arrows in the control and mutant samples indicate Claudin-3 signal in the skin overlying the brain. Double-arrows indicate Claudin-3-/IB4+ vessels in the *Rdh10* mutants. (E) Arrows indicate LEF-1+ (green) ECs (Ib4 in red) in the neocortex of *Bat-gal-LacZ/+* and *Rdh10 mutant; Bat-gal-LacZ/+* animals. (F) Quantitative PCR for transcript expression of WNT ligands (*Wnt7a, Wnt7b*) and WNT inhibitors (*Sfrp1, Sfrp2, Sfrp5,* and *Dkk1*) in wildtype and *Rdh10* mutant E13.5 neocortices and non-neocortical brain structures. Asterisks indicate significance between control and *Rdh10* mutants. (G) Quantitative PCR for transcription expression of the WNT inhibitors *Sfrp5 and Dkk1* in cultured neocortical progenitors treated with RA or a pan RAR inhibitor. # indicates significance from vehicle. Scale bars are 100 µm.

Figure 4. Elevated WNT signaling in non-cortical *Rdh10* mutant vasculature and neurovascular development in *PdgfbiCre; dnRAR403-flox* animals

(A) β-galactosidase (β-gal: green) and Ib4 (red) co-immunolabeling in the thalamic vasculature of E14.5 *Bat-gal-LacZ/+* and *Rdh10* mutant*; Bat-gal-LacZ/+* animals. Open arrows indicate β-gal+ ECs. (B)

Top: Depiction of pre-natal tamoxifen injection timing for *PdgfbiCre; dnRAR403-flox* animals. Bottom: GFP (green) immunostaining and Ib4 (red) labeling in E14.5 *PdgfbiCreER^{T2}-IRES-GFP* (aka *PdgfbiCre*) brain to illustrate specific expression of transgene in blood vessels. Arrows indicate GFP+/Ib4+ blood vessels, open arrows indicate GFP-/Ib4+ microglia. (C) Whole fetus images of E18.5 control (*dnrar403-fl/+*), and mutant (*PdgfbiCre; dnrar403-fl/+* or *fl/fl*). (D) Low magnification image of whole brains from *PdgfbiCre/+* animals with 0 or 2 copies of the *dnRAR403-flox* allele. Arrows indicate hemorrhage within the cerebral hemispheres (CH). (E) GLUT-1 (green), Ib4 (red) and DAPI stained cortical sections of E18.5 *PdgfbiCre/+* and *PdgfbiCre; dnRAR403-fl/fl* mutant. Open arrows indicate micro-hemorrhages. Inset shows GLUT-1+ red blood cells in the brain parenchyma, indicative of hemorrhage. Arrow in inset indicates activated Ib4+ microglia with amoeboid morphology. (F) Ib4+ cerebrovasculature in E18.5 *PdgfbiCre/+* and *PdgfbiCre; dnRAR403-fl/fl* mutant sections. Arrows indicate enlarged vessels in mutant sample. (G) Neocortical progenitor markers Pax6, Tbr2 and deep layer cortical neuronal marker Ctip2 in E16.5 *PdgfbiCre/+* and *PdgfbiCre; dnRAR403-fl/fl* mutant sections. Scale bars = 100 µm (A & G) and 200 µm (E & F).

<u>Figure 5. Endothelial WNT signaling in increased in fetal brain vasculature of *PdgfbiCre; dnRAR403-flox* mutants</u>

(A, B) Open arrows indicate β-gal+ (green), Ib4+ (red) ECs in the striatum of E18.5 *PdgfbiCre/+; Bat-gal-LacZ/+* and *PdgfbiCre; dnRAR403-fl/fl; Bat-gal-lacZ/+*. (C) Graph depicting quantification of β-gal+ ECs per vessel length in E18.5 control (*PdgfbiCre/+; Bat-gal-LacZ/+* or *dnRAR403-flox;Bat-gal-LacZ/+*) and mutant (*PdgfbiCre; dnRAR403-fl/+; Bat-gal-lacZ/+*, *PdgfbiCre; dnRAR403-fl/fl; Bat-gal-lacZ/+*) cortical, striatal and thalamic vasculature. Asterisk indicates significance from control, # indicates significance from *PdgfbiCre; dnRAR403-fl/+*. (D, E) LEF-1 (green), Ib4+ (red) ECs in the neocortex of *PdgfbiCre/+* and *PdgfbiCre; dnRAR403-fl/fl.* (F) LEF-1 (54 kDa), and β-actin (52 kDa)

immunoblots on protein lysate from E18.5 control (□: *PdgfbiCre/+* or *dnRAR403-flox)* or mutant (■: *PdgfbiCre; dnRAR403-fl/fl*) neocortices. (G) LEF-1 (green) and Ib4 (red) immunofluorescence in the head area of E18.5 *PdgfbiCre/+* and *PdgfbiCre; dnRAR403-fl/fl* animals. Arrows indicate Ib4+/LEF-1- vessels. Scale bars are 100 µm.

Figure 6. RA inhibits endothelial WNT signaling in vivo and in vitro.

(A) Depiction of RA treatment paradigm for pregnant *Bat-gal-LacZ/+* animals. (B) Graph depicting quantification of β-gal+ ECs per 100 µm vessel length in control and RA exposed fetuses at E14.5 and E16.5. Asterisk indicates statistically significant difference from E14.5, control diet. # indicates statistically significant difference from control diet at E16.5. (C) Graph depicting quantification of vessel density in control and RA diet treated animals at E14.5 and E16.5. (D) Graph depicting quantification of transwell migration assay with bEnd.3 cell line following treatment with RA, WNT3a or RA+WNT3a. Asterisks indicate significance from untreated cells (CTL). (E) Quantification of cell proliferation of bEnd.3 cells following a 3 day treatment of RA, WNT3a or both treatments. Asterisks indicate significance from untreated cells (CTL). # indicates statistically significant difference from WNT3a treatment. (F) RT-PCR for *RAR*s and *RXR*s using E18.5 microvessel and postnatal day 7 meninges cDNA. Housekeeping gene GAPDH is used to show equal amount of RNA to generate the cDNA used in the RT-PCR reaction. (G) Transfection of a RARα construct decreases the response of cells to WNT stimulation. Two way ANOVA revealed a significant difference due to construct ($F_{(1,16)}$ =1301, $p<0.001$) and treatment ($F_{(3,16)}$ =518.1, $p<0.001$), as well as a significant interaction between both factors ($F_{(3,16)}$ =200.1, $p<0.001$). (H) RXRβ does not alter the response of cells to WNT stimulation. Two way ANOVA revealed a significant difference due to treatment ($F_{(3,16)}$ =90.17, $p<0.001$), but no significant difference due to construct ($F_{(1,16)}$ =4.358, $p>0.05$) or interaction between the two factors ($F_{(3,16)}$ =1.188, $p>0.05$). (I) dnRARα increases the response of cells to WNT stimulation.

Two way ANOVA revealed a significant difference due to construct ($F_{(1,16)}$ =110.7, p<0.001) and treatment ($F_{(3,16)}$ =110.7, p<0.001), as well as a significant interaction between the two factors ($F_{(3,16)}$ =49.98, p<0.001). For G-I, asterisks directly above the bar indicate significance from untreated pCIG control and hash marks indicate significance from WNT3a treatment alone; within group differences are indicated by connected lines.

Figure 7. Elevated expression of Sox17 in *PdgfbiCre; dnRAR403-fl/fl* neurovasculature.

(A) Immunostaining for Sox17 (green) in Ib4+ (red) cerebral vessels in tissue from control and an EC-specific knockdown of WNT signaling component β-catenin at E14.5 (*PdgfbiCre; Ctnnb1-fl/fl*). (B) Graph depicting *Lef1*, *Axin2*, and *Sox17* transcript levels in microvessels isolated from E18.5 *PdgfbiCre/+;Ctnnb1-fl/+* and *PdgfbiCre/+; Ctnnb1-fl/fl* brains. Asterisks indicate significance from *PdgfbiCre;Ctnnb1-fl/+* value. (C) Representative Sox17 (green) immunostaining in Ib4+ (red) cerebral vessels at E18.5 from *PdgfbiCre/+* and *PdgfbiCre; dnRAR403-fl/fl* brains. Open arrows indicate weakly Sox17+ vessels, arrows indicate vessels with high Sox17 expression. (D) Sox17 (44 kDa) and β-actin (52 kDa) immunoblots on protein lysate from E18.5 control (□: *PdgfbiCre/+* or *dnRAR403-flox)* or mutant (■: *PdgfbiCre; dnRAR403-fl/fl*) neocortices. Scale bars are 100 µm.

Figure 8. Elevated Sox17 expression in *PdgfbiCre; dnRAR403-fl/fl* venous and arterial vessels.

(A, B) Immunostaining for Sox17 (green) and Coup-TFII (red) on E18.5 *PdgfbiCre/+* (A) and *PdgfbiCre; dnRAR403-fl/fl* (B) brains. Open arrows indicate Ib4+ (blue) vessels with Coup-TFII+ ECs (presumptive venous blood vessel). Arrow in A indicates blood vessel in control brain tissue that is Coup-TFII-/Sox17+ (presumptive arterial vessel). Double arrows indicate Coup-TFII+ mural cells, triple arrow indicates Coup-TFII+ neural cell. (C, D) GFP (red) and Sox17 (green) immunostaining in control and *PdgfbiCre; dnRAR403-fl/fl* animals expressing *Ephrin B2-GFP* that labels arterial EC nuclei. Arrows indicate GFP+/Sox17+ arterial EC nuclei and open arrows indicate Sox17 expression in GFP-

EC nuclei. C" and D" show overlay with Ib4 to label the vasculature (blue). *Ephrin-B2-GFP* is also expressed by some neurons (double-head arrow). GFP IF is present in endothelial cell membrane of D images due to IRES-GFP present in *PdgfbiCre* allele construct (triple-arrow). Scale bars are 100 µm.

Figure 9. Model of RA functions during brain vascular development

(A) RA in the developing neocortex normally functions to suppress expression of WNT inhibitors (Dkk1, sFRPs) to create a permissive environment for endothelial WNT signaling that drives cerebrovascular development. In RA-deficient *Rdh10* mutants, ectopic expression of WNT inhibitors impedes endothelial WNT signaling which disrupts growth of the cerebrovasculature. (B) RA functions cell autonomously in brain endothelial cells (ECs), likely through its receptor RARα, to inhibit WNT-β-catenin transcriptional and limit expression of its target gene Sox17.

Figure 1

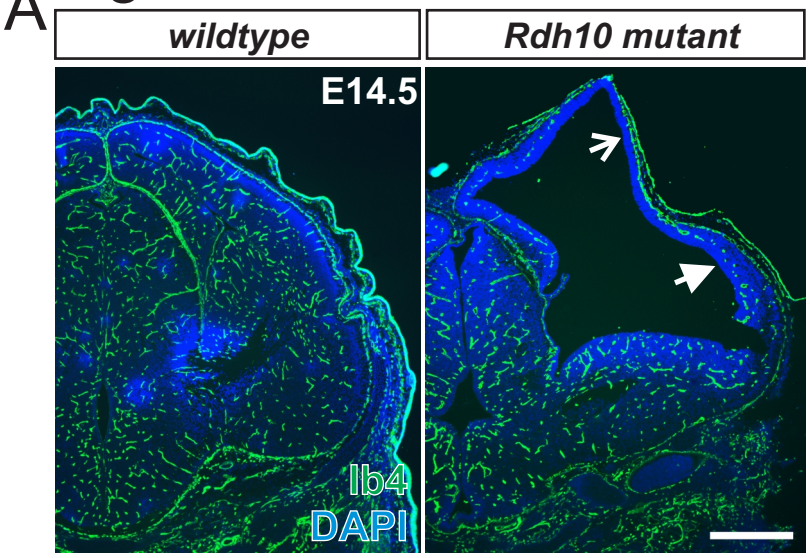
A
wildtype
Rdh10 mutant
E14.5
Ib4
DAPI

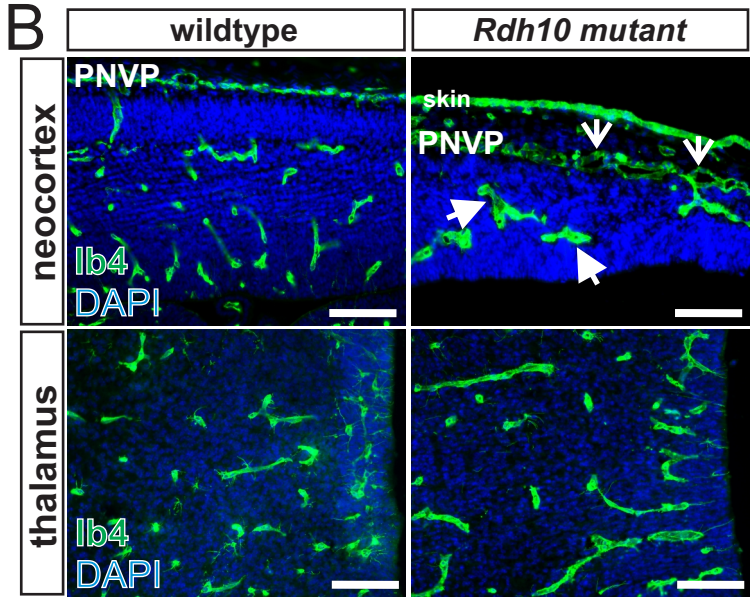
B
wildtype
Rdh10 mutant
neocortex
thalamus
PNVP
skin
Ib4
DAPI

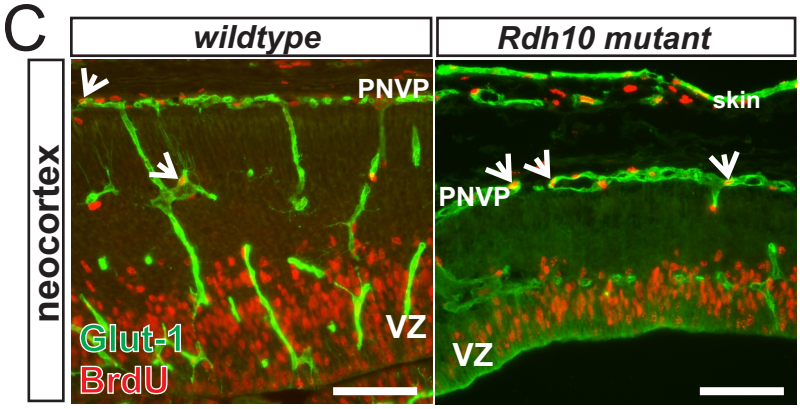
C
wildtype
Rdh10 mutant
neocortex
PNVP
skin
VZ
Glut-1
BrdU

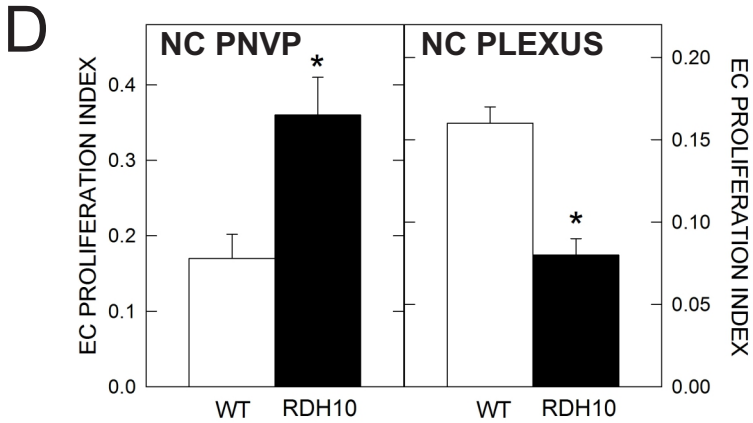
D
NC PNVP
NC PLEXUS
EC PROLIFERATION INDEX
0.0
0.1
0.2
0.3
0.4
0.00
0.05
0.10
0.15
0.20
WT
RDH10
*

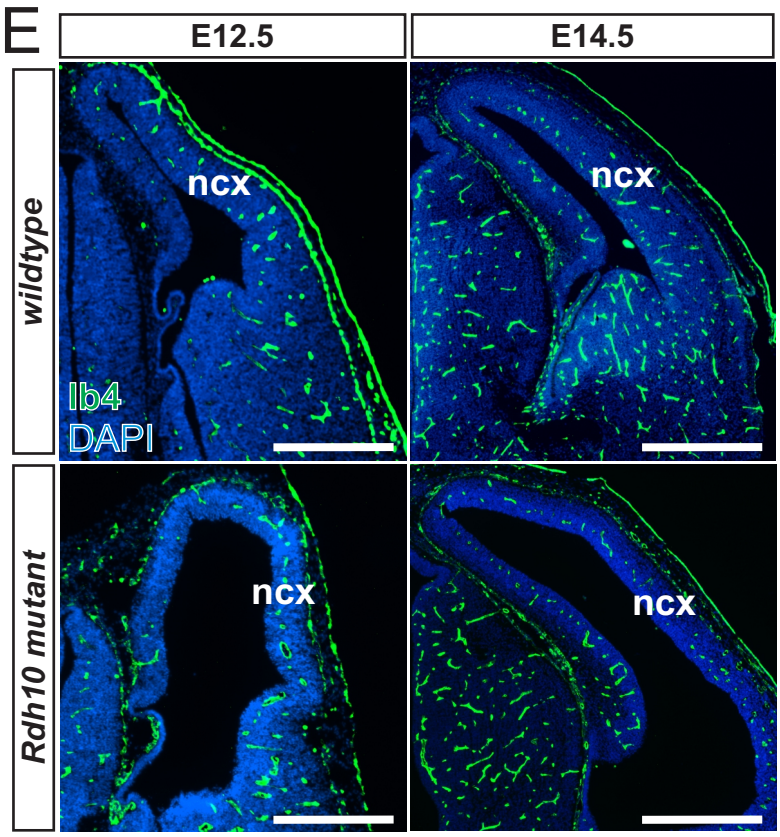
E
E12.5
E14.5
wildtype
Rdh10 mutant
ncx
Ib4
DAPI

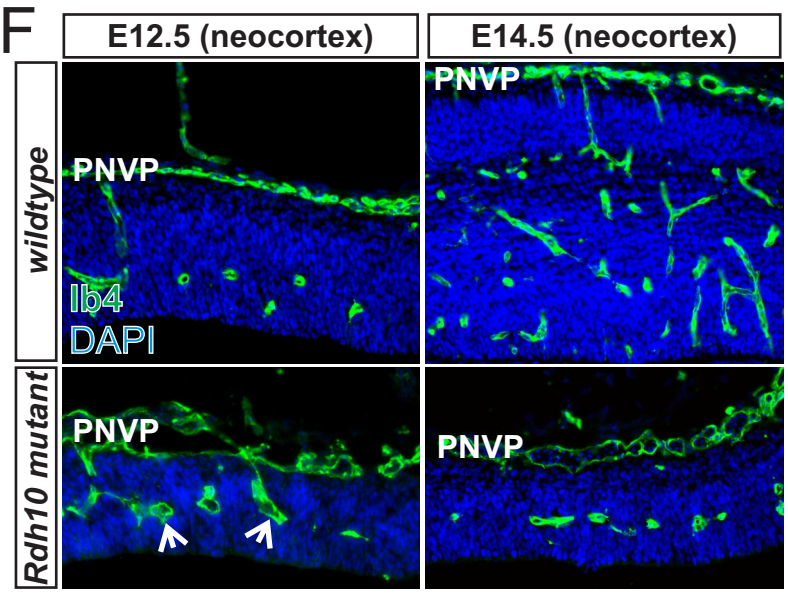
F
E12.5 (neocortex)
E14.5 (neocortex)
wildtype
Rdh10 mutant
PNVP
Ib4
DAPI

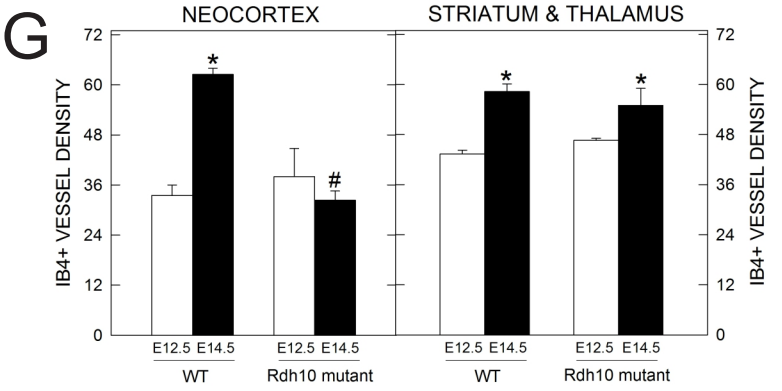
G
NEOCORTEX
STRIATUM & THALAMUS
IB4+ VESSEL DENSITY
0
12
24
36
48
60
72
E12.5 E14.5
WT
Rdh10 mutant
*
#

Figure 2

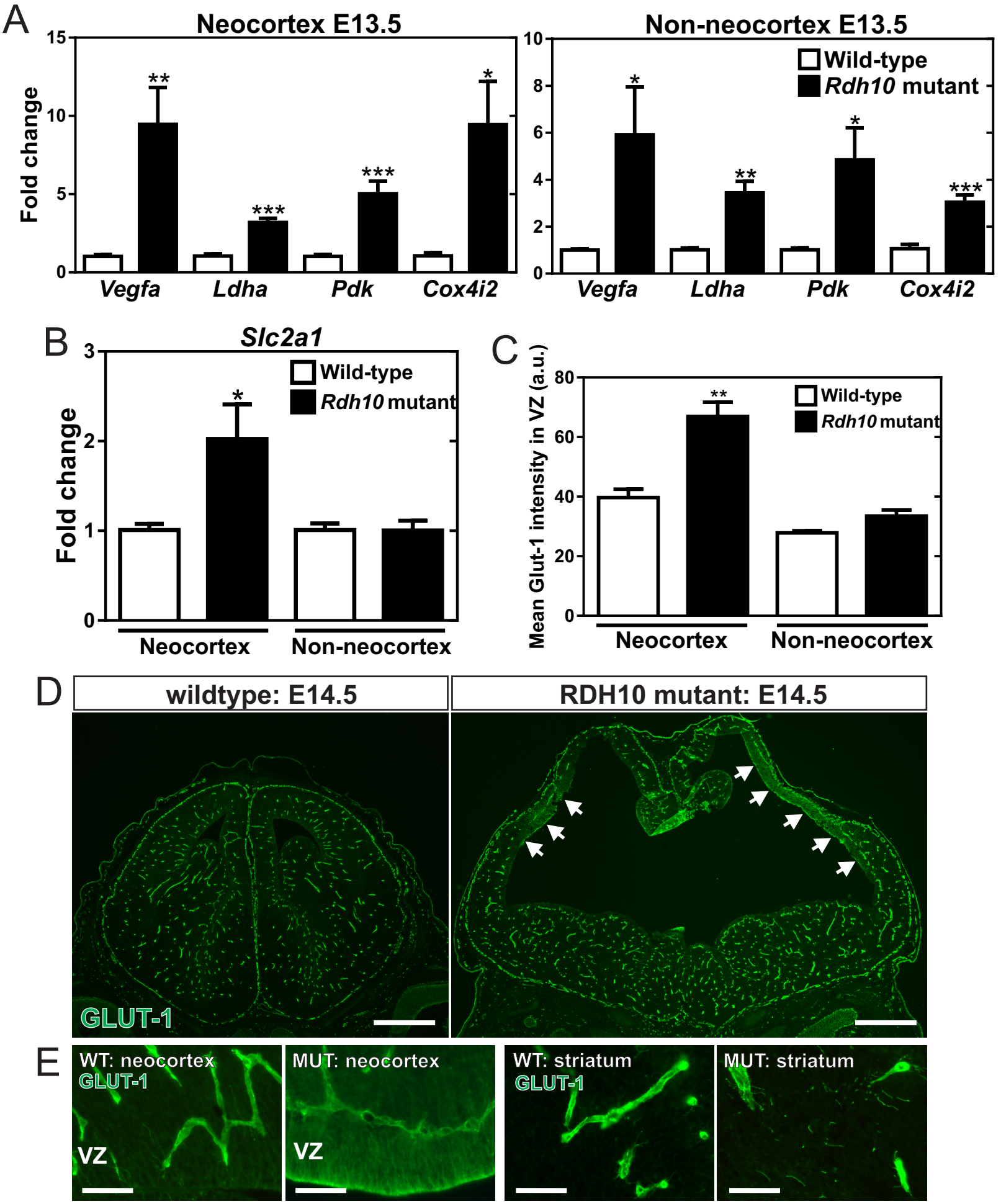
A
Neocortex E13.5
Non-neocortex E13.5
Fold change
Wild-type
Rdh10 mutant
Vegfa
Ldha
Pdk
Cox4i2
B
Slc2a1
Fold change
Wild-type
Rdh10 mutant
Neocortex
Non-neocortex
C
Mean Glut-1 intensity in VZ (a.u.)
Wild-type
Rdh10 mutant
Neocortex
Non-neocortex
D
wildtype: E14.5
RDH10 mutant: E14.5
GLUT-1
E
WT: neocortex
GLUT-1
VZ
MUT: neocortex
VZ
WT: striatum
GLUT-1
MUT: striatum

Figure 3

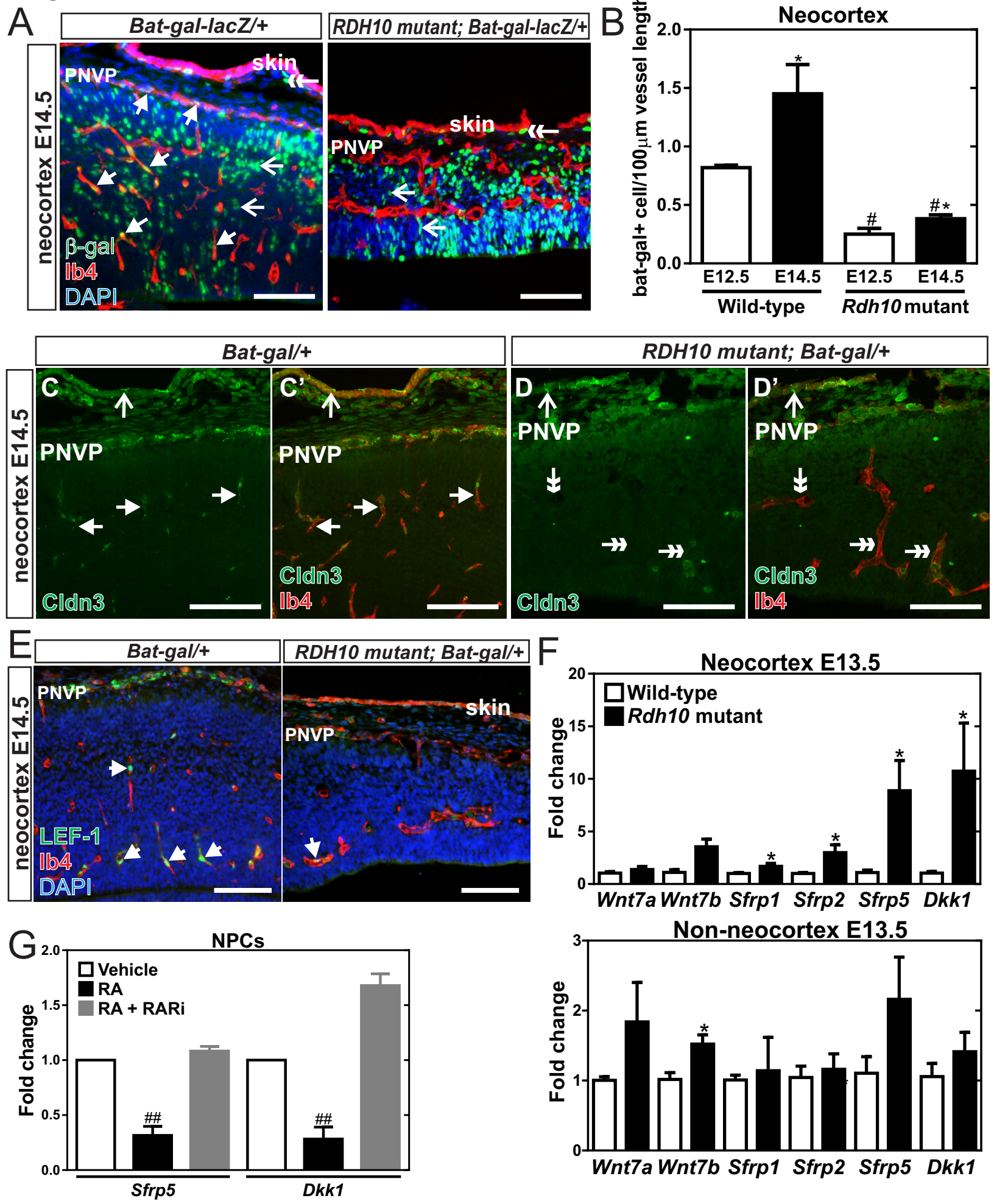
A
Bat-gal-lacZ/+
RDH10 mutant; Bat-gal-lacZ/+
neocortex E14.5
PNVP
skin
β-gal
Ib4
DAPI
B
Neocortex
bat-gal+ cell/100μm vessel length
2.0
1.5
1.0
0.5
0.0
E12.5
E14.5
E12.5
E14.5
Wild-type
Rdh10 mutant
Bat-gal/+
RDH10 mutant; Bat-gal/+
C
C'
D
D'
Cldn3
Ib4
E
LEF-1
F
Neocortex E13.5
Wild-type
Rdh10 mutant
Fold change
Wnt7a
Wnt7b
Sfrp1
Sfrp2
Sfrp5
Dkk1
Non-neocortex E13.5
G
NPCs
Vehicle
RA
RA + RARi
Sfrp5
Dkk1

Figure 4

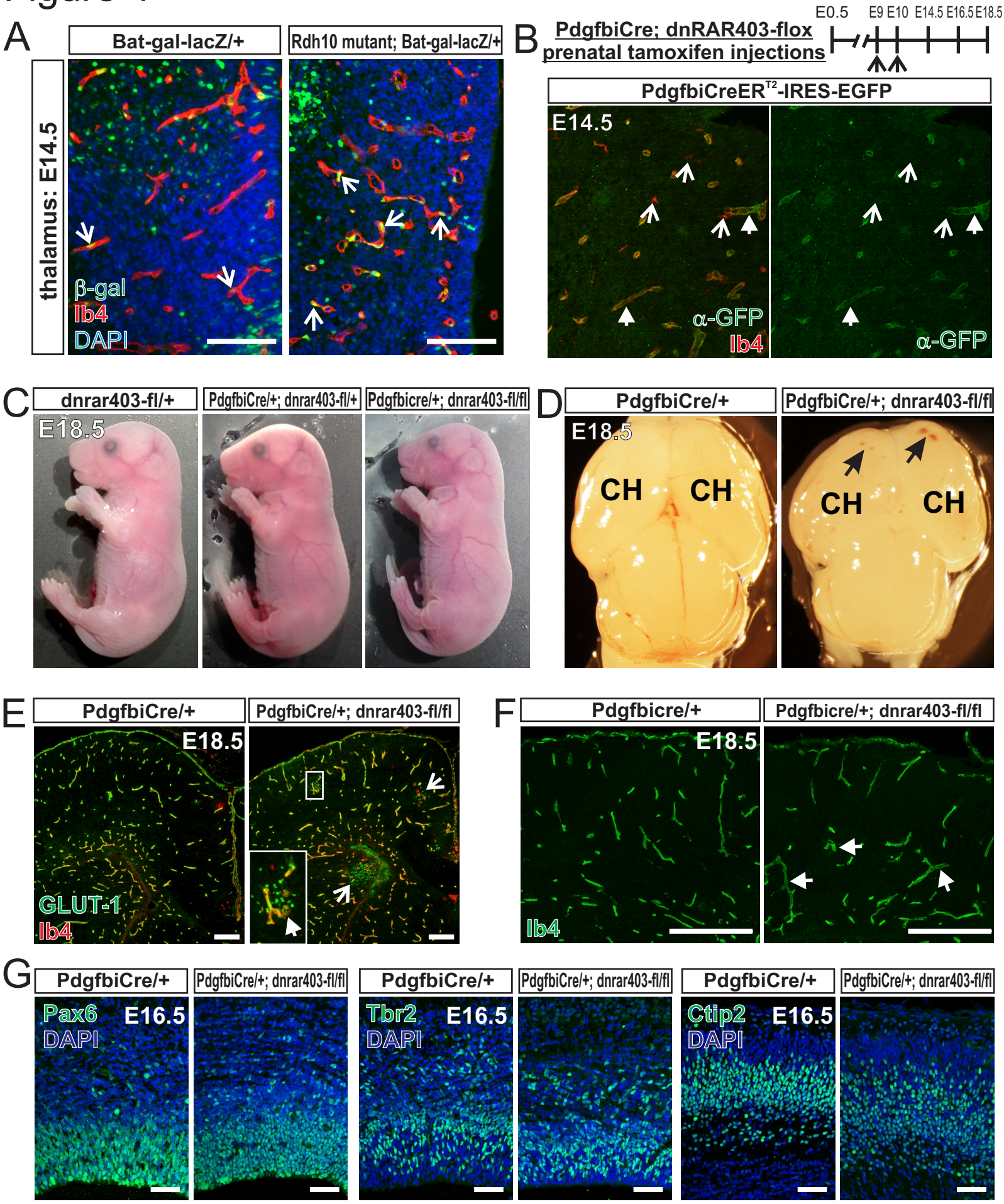
A
Bat-gal-lacZ/+
Rdh10 mutant; Bat-gal-lacZ/+
thalamus: E14.5
β-gal
Ib4
DAPI
B
PdgfbiCre; dnRAR403-flox
prenatal tamoxifen injections
E0.5
E9 E10
E14.5 E16.5 E18.5
PdgfbiCreER^{T2}-IRES-EGFP
E14.5
α-GFP
Ib4
α-GFP
C
dnrar403-fl/+
PdgfbiCre/+; dnrar403-fl/+
Pdgfbicre/+; dnrar403-fl/fl
E18.5
D
PdgfbiCre/+
PdgfbiCre/+; dnrar403-fl/fl
E18.5
CH
CH
CH
CH
E
PdgfbiCre/+
PdgfbiCre/+; dnrar403-fl/fl
E18.5
GLUT-1
Ib4
F
Pdgfbicre/+
Pdgfbicre/+; dnrar403-fl/fl
E18.5
Ib4
G
PdgfbiCre/+
PdgfbiCre/+; dnrar403-fl/fl
Pax6
DAPI
E16.5
PdgfbiCre/+
PdgfbiCre/+; dnrar403-fl/fl
Tbr2
DAPI
E16.5
PdgfbiCre/+
PdgfbiCre/+; dnrar403-fl/fl
Ctip2
DAPI
E16.5

Figure 5

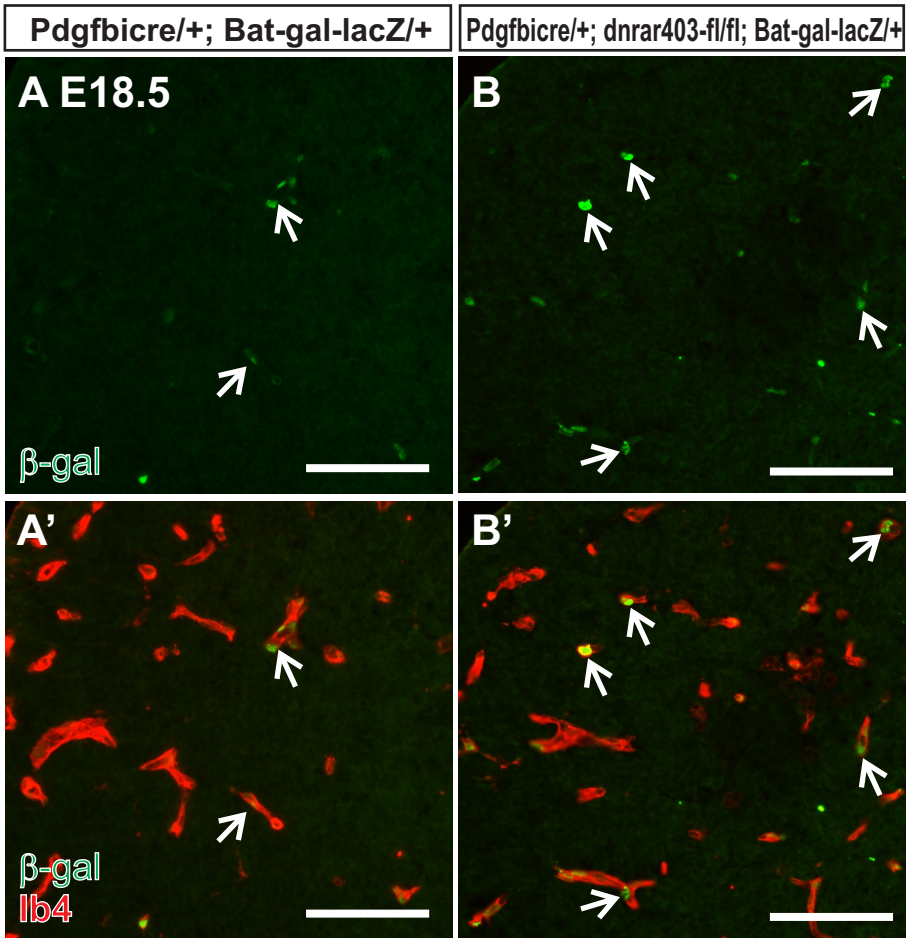
Pdgfbicre/+; Bat-gal-lacZ/+
Pdgfbicre/+; dnrar403-fl/fl; Bat-gal-lacZ/+
A E18.5
B
β-gal
A'
B'
β-gal
Ib4

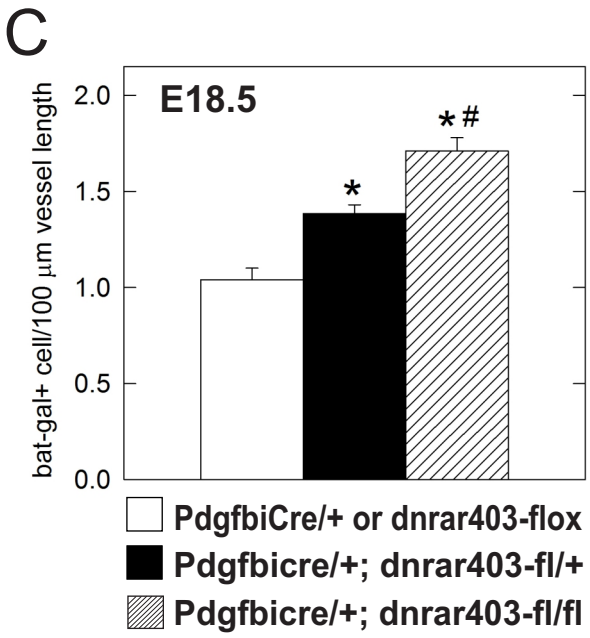
C
E18.5
bat-gal+ cell/100 μm vessel length
2.0
1.5
1.0
0.5
0.0
*
*#
PdgfbiCre/+ or dnrar403-flox
Pdgfbicre/+; dnrar403-fl/+
Pdgfbicre/+; dnrar403-fl/fl

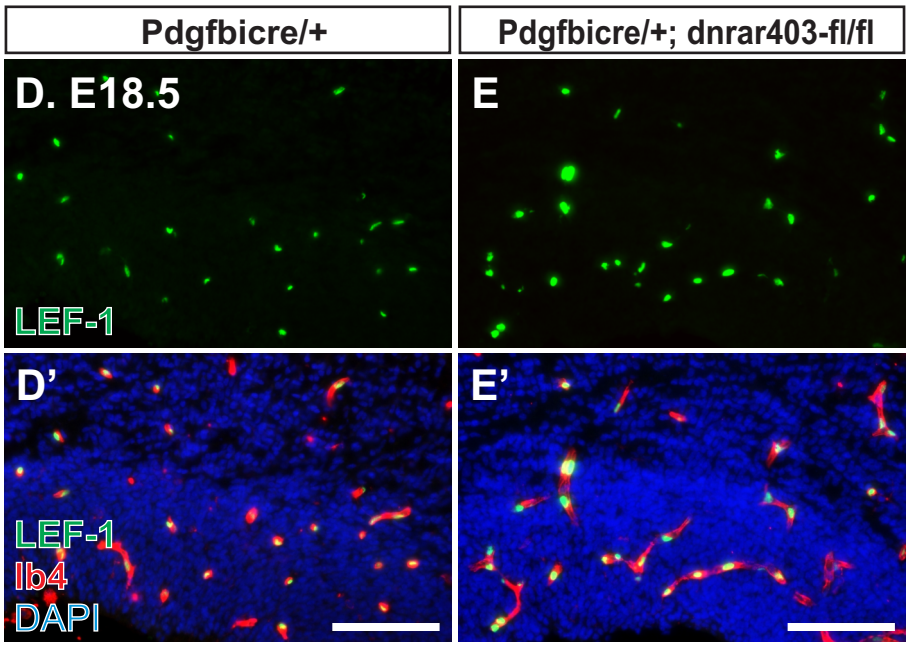
Pdgfbicre/+
Pdgfbicre/+; dnrar403-fl/fl
D. E18.5
E
LEF-1
D'
E'
LEF-1
Ib4
DAPI

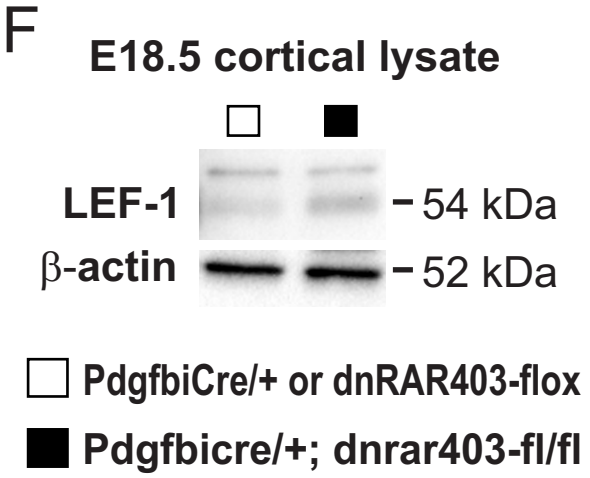
F
E18.5 cortical lysate
LEF-1
β-actin
54 kDa
52 kDa
PdgfbiCre/+ or dnRAR403-flox
Pdgfbicre/+; dnrar403-fl/fl

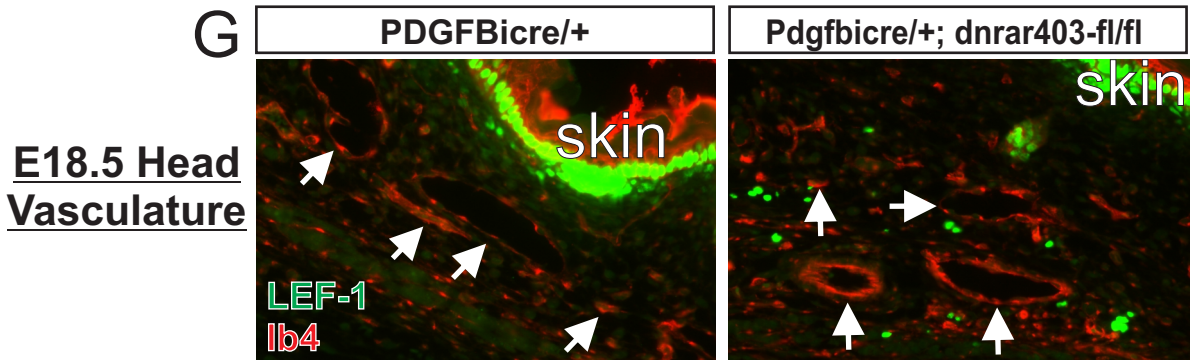
G
E18.5 Head Vasculature
PDGFBicre/+
Pdgfbicre/+; dnrar403-fl/fl
skin
skin
LEF-1
Ib4

Figure 6

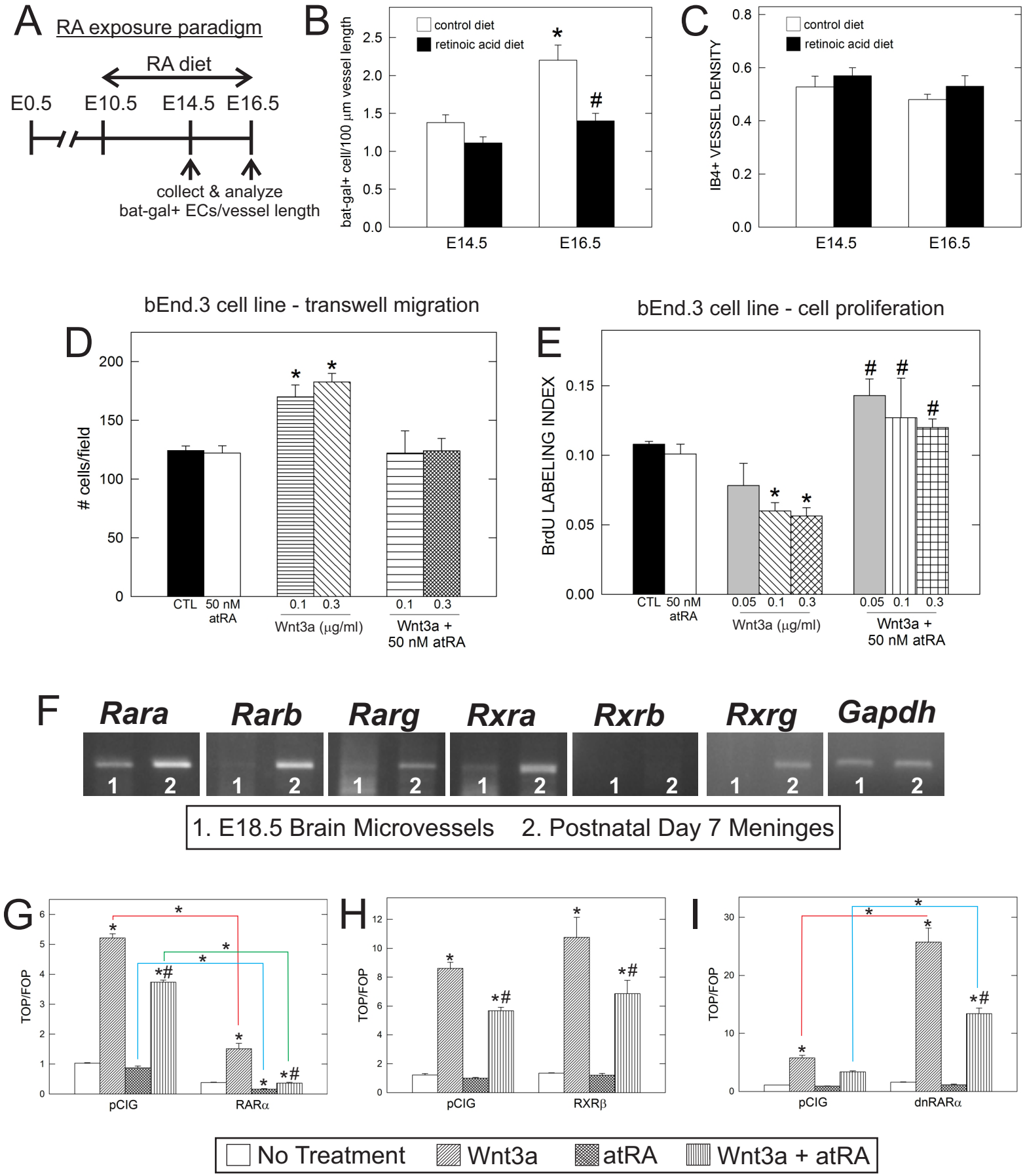
A
RA exposure paradigm
RA diet
E0.5
E10.5
E14.5
E16.5
collect & analyze
bat-gal+ ECs/vessel length
B
control diet
retinoic acid diet
bat-gal+ cell/100 μm vessel length
E14.5
E16.5
C
control diet
retinoic acid diet
IB4+ VESSEL DENSITY
E14.5
E16.5
bEnd.3 cell line - transwell migration
D
cells/field
CTL
50 nM atRA
0.1
0.3
Wnt3a (μg/ml)
Wnt3a + 50 nM atRA
bEnd.3 cell line - cell proliferation
E
BrdU LABELING INDEX
CTL
50 nM atRA
0.05
0.1
0.3
Wnt3a (μg/ml)
Wnt3a + 50 nM atRA
F
Rara
Rarb
Rarg
Rxra
Rxrb
Rxrg
Gapdh
1. E18.5 Brain Microvessels
2. Postnatal Day 7 Meninges
G
TOP/FOP
pCIG
RARα
H
TOP/FOP
pCIG
RXRβ
I
TOP/FOP
pCIG
dnRARα
No Treatment
Wnt3a
atRA
Wnt3a + atRA

Figure 7

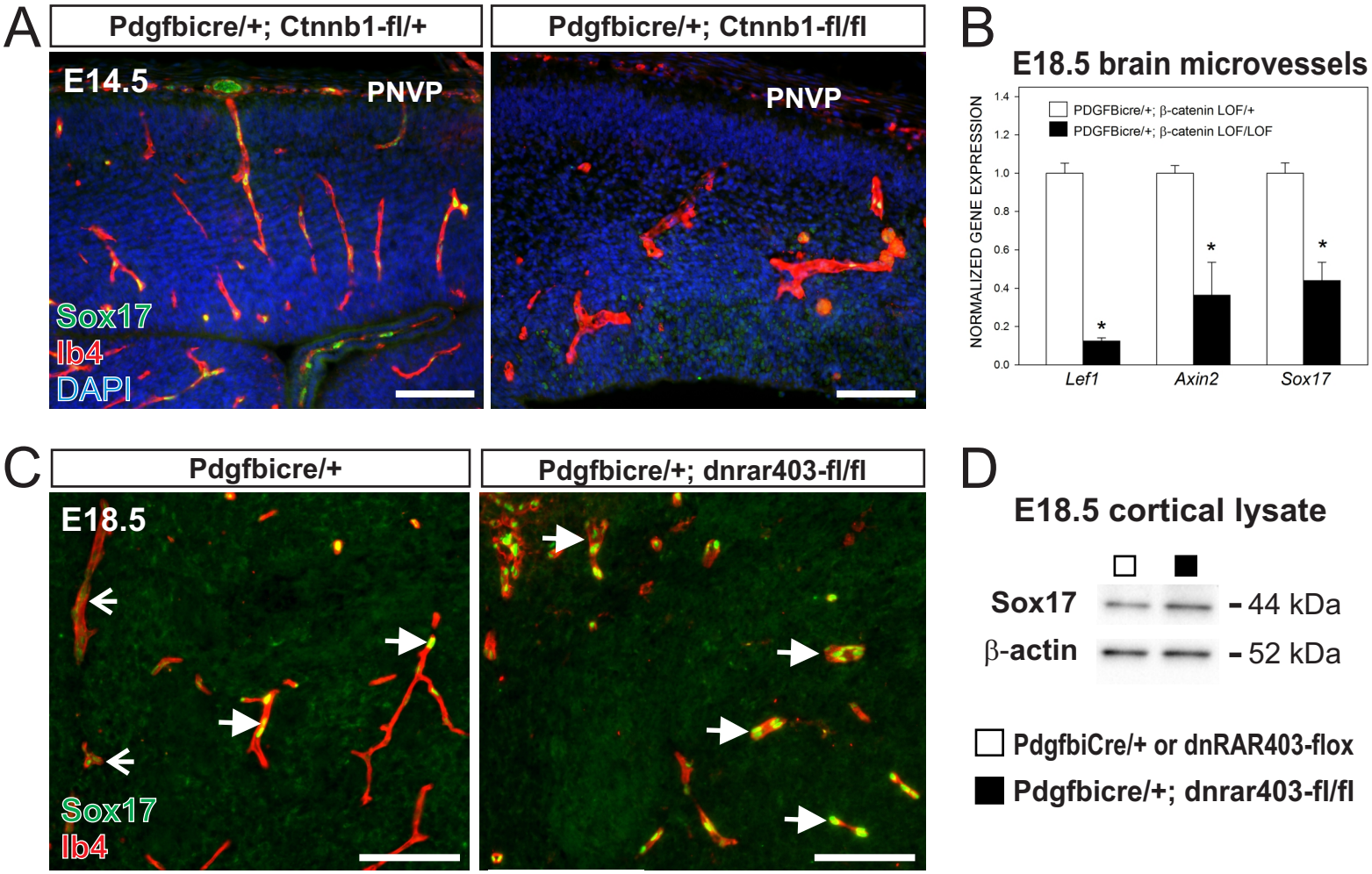
A
Pdgfbicre/+; Ctnnb1-fl/+
Pdgfbicre/+; Ctnnb1-fl/fl
E14.5
PNVP
PNVP
Sox17
Ib4
DAPI
B
E18.5 brain microvessels
NORMALIZED GENE EXPRESSION
PDGFBicre/+; β-catenin LOF/+
PDGFBicre/+; β-catenin LOF/LOF
1.4
1.2
1.0
0.8
0.6
0.4
0.2
0.0
Lef1
Axin2
Sox17
C
Pdgfbicre/+
Pdgfbicre/+; dnrar403-fl/fl
E18.5
Sox17
Ib4
D
E18.5 cortical lysate
Sox17
β-actin
44 kDa
52 kDa
PdgfbiCre/+ or dnRAR403-flox
Pdgfbicre/+; dnrar403-fl/fl

Figure 8

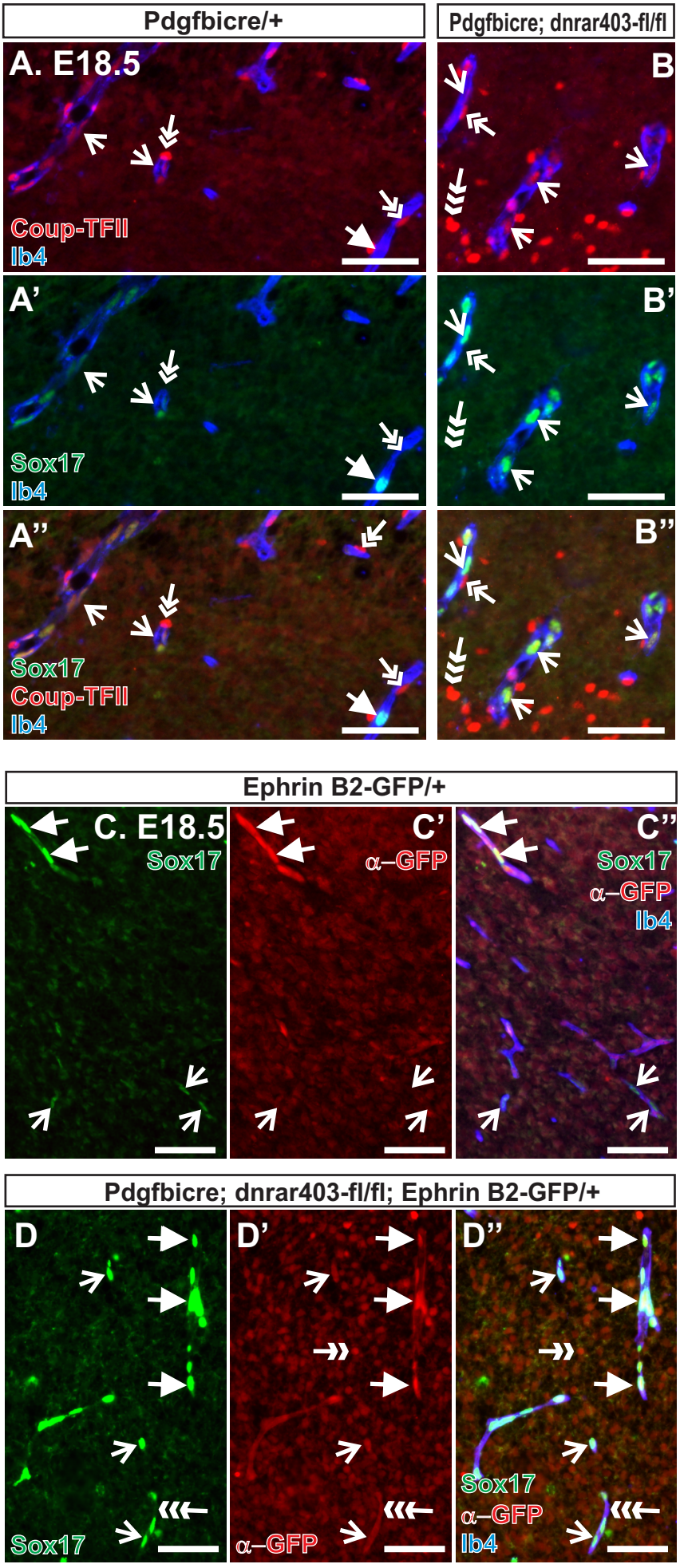
Pdgfbicre/+
Pdgfbicre; dnrar403-fl/fl
A. E18.5
Coup-TFII
Ib4
B
A'
Sox17
Ib4
B'
A''
Sox17
Coup-TFII
Ib4
B''
Ephrin B2-GFP/+
C. E18.5
Sox17
C'
α–GFP
C''
Sox17
α–GFP
Ib4
Pdgfbicre; dnrar403-fl/fl; Ephrin B2-GFP/+
D
Sox17
D'
α–GFP
D''
Sox17
α–GFP
Ib4

Figure 9

A. RA in cerebrovascular development: non-cell autonomous function in regulating WNT inhibitors

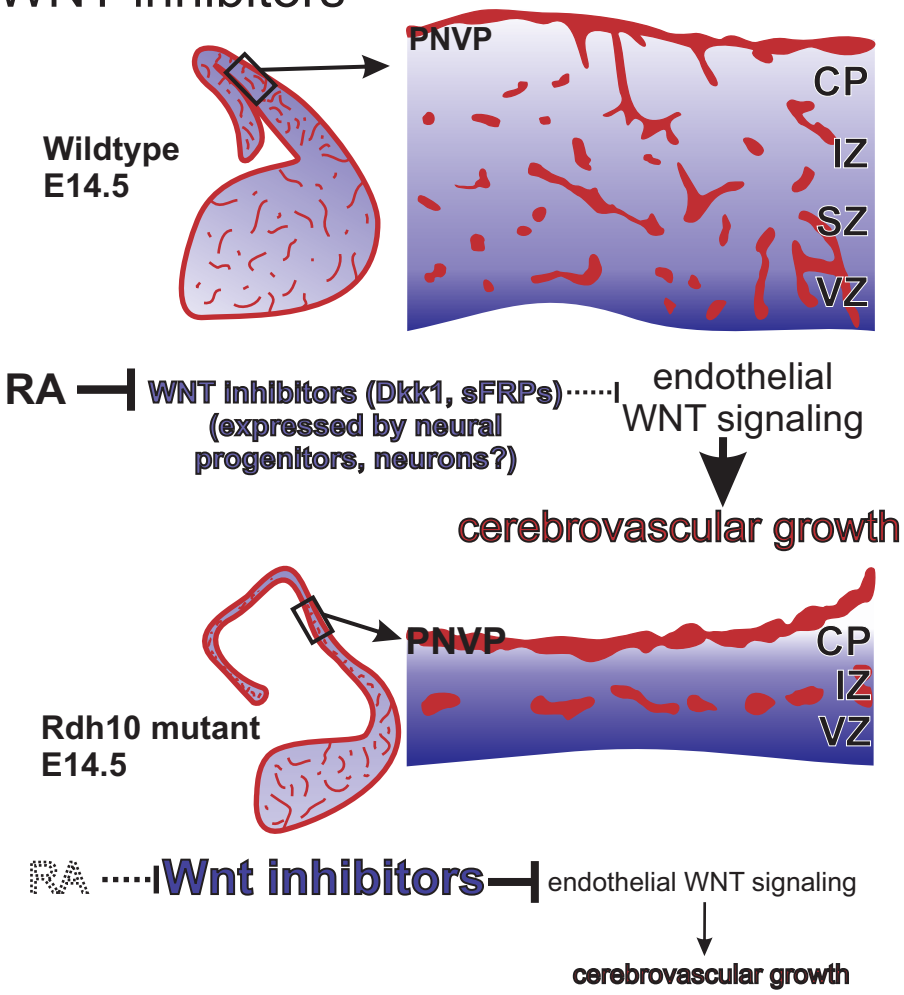

B. RA signaling in brain endothelial cells: cell autonomous modulation of WNT transcriptional activity